Report UAH-QERL-92-1

FINAL REPORT

MATERIALS CHARACTERIZATION ON EFFORTS FOR ABLATIVE MATERIALS

By

Thomas P. Tytula
Kristin C. Schad
Myles H. Swann

Contract NAS8-38609,
Delivery Order 3

September, 1992

NASA

Report Documentation Page

1. Report No.	2. Government Accession No.	3. Recipient's Catalog No.

4. Title and Subtitle

Materials Characterization on Efforts for Ablative Materials

5. Report Date

September, 1992

6. Performing Organization Code

7. Author(s)

Thomas P. Tytula, Kristin C. Schad, Myles H. Swann

8. Performing Organization Report No.

UAH-QERL-92-1

10. Work Unit No.

9. Performing Organization Name and Address

The University of Alabama in Huntsville
Huntsville, AL 35899

11. Contract or Grant No.

Contract NAS8-38609
D.O. 3

13. Type of Report and Period Covered

Final Report

12. Sponsoring Agency Name and Address

National Aeronautics and Space Administration
George C. Marshall Space Flight Center, Alabama 35812

14. Sponsoring Agency Code

15. Supplementary Notes

16. Abstract

Experimental efforts to develop a new procedure to measure char depth in carbon phenolic nozzle material are described. Using a Shor Type D Durometer, hardness profiles were mapped across post fired sample blocks and specimens from a fired rocket nozzle. Linear regression was used to estimate the char depth. Results are compared to those obtained from computed tomography in a comparative experiment. There was no significant difference in the depth estimates obtained by the two methods.

17. Key Words (Suggested by Author(s))	18. Distribution Statement
Char depth, carbon phenolic, hardness testing, designed experimentation	Unclassified - unlimited

19. Security Classif. (of this report)	20. Security Classif. (of this page)	21. No. of pages	22. Price
Unclassified	Unclassified	51	

Table of Contents

Figures

Tables

I. INTRODUCTION

The objectives of this task were to develop a procedure for measurement of char and erosion in ablative materials, to develop an optimal procedure for use of the Marshall Space Flight Center (MSFC) plasma asher facility and to analyze the resulting data for char monitoring. Also included were the design of experiments, testing, statistical data analysis, and characterization of existing procedures for measuring char and erosion in materials. The bulk of the effort involved the measurement of char depth in carbon phenolic material. A new procedure for measuring char depth was developed and shown to provide estimates of char depth to an accuracy equivalent to that obtained by Computed Tomography, the most objective method heretofore available.

Carbon phenolic, a carbonized, resin impregnated cloth, is used as an insulator in solid rocket motor nozzles. It is a rigid material, capable of withstanding high temperatures, particulate impact, and erosive chemical environments. It insulates by ablative action, progressively heating, charring, and flaking away the charred layers. It is a very dense material and thus it is very heavy. In its rocket nozzle application it is desirable to minimize the weight of material used; hence, there is wide interest in efficient, inexpensive, and accurate measurement of the location of the boundary between virgin material and charred material.

Initial efforts concentrated on generating an operational definition of char; e.g., a procedure and resulting attributes that could be used to say "this is char" and "this is not char." Discussions with various personnel at MSFC revealed a general lack of agreement on what constituted char. Nevertheless, the one common characteristic seemed to involve density. Density loss is a consistent characteristic of charred carbon phenolic.

A review of previous efforts in this area, together with current practice, revealed that there were three basic methods for estimating the char boundary location. One method was visual, where the fired material is physically sectioned and either scratched or sprayed with lacquer. When scratched, the less dense, charred region will appear dull. Likewise, when sprayed the less dense, more porous material absorbs the lacquer and a visible boundary appears. The location of this boundary can then be measured and mapped onto a permanent record. In the case of the scratch method, the outline of the fired material and the visual boundary are frequently traced onto a mylar sheet from which the measurements are taken; hence the name "slice-mylar" for this procedure.

The second method involves carefully sectioning the fired material, measuring its dimensions, and weighing it. A small increment, typically 20 mils thick, is then milled from the heat affected region and the sample again measured and weighed. The bulk density of the original and milled sample are calculated, the difference being an estimate of the density of the removed material. The process is then repeated until the density of the removed material stabilizes, indicating virgin material, and the density profile is mapped. From this profile, the boundary between virgin and heat affected material can be estimated using regression techniques described below.

The third method uses Computed Tomography (CT) to map the interior of the fired specimen. The resultant output is recorded as CT numbers, which can be used to construct a profile of CT number versus distance on any plane through the specimen. It has been shown that CT number is highly correlated with bulk density, and that CT profiles when corrected for oxygen and nitrogen profiles, provide accurate estimates of bulk density in carbon phenolic [1].

In order to define the char boundary, a linear estimating relationship is defined for each of the heat affected and virgin regions of the CT number profile. The intersection of these two linear functions is taken as the operational definition of the char boundary. Thus, the boundary is defined by the onset of pyrolysis. This technique is described by Northrup [2].

Little of additional value was found during an extensive review of the literature. A brief annotated bibliography was provided in Quarterly Report 1 for this task. Most notable of these was the work of Ikeda, Yamamoto, and M. Kohno [3] which verified the correspondence between CT number and bulk density gradients.

Both CT and direct density measurements require time consuming, tedious data gathering. With CT, special equipment is required and special training is necessary to operate it. The results obtained are objective and it has the advantage of being nondestructive. Hence, material characteristics are not altered and there is complete flexibility with respect to the conduct of additional tests after CT. The direct density measurement is also an objective technique; however, it requires relatively precise measurements and destroys the specimen in the process. The visual techniques are simple, but they suffer from lack of objectivity. Northrup [2] showed that the error in measurements could be as high as 29%. She also points out the possible influence of observer biases. As a consequence, CT has been the method of choice for measuring char depth up to now.

Three additional techniques for locating the char boundary were investigated during this task. These were x-ray, microscopic examination, and hardness mapping. The first two were dropped from further contention early because of their lack of promise. Hardness mapping showed substantial promise and was investigated in detail. The rest of this report documents these investigations and their associated results.

The hardness investigation was conducted in three parts. The firs part examined the feasibility of using hardness measurements to determine the char boundary location. It was conducted using sample blocks from different manufacturers which were charred in the plasma asher facility at MSFC. In addition, it specifically examined operator influence as an experimental variable. The next section describes this effort and the associated results.

Part two again used the sample blocks which were charred in the plasma asher. It attempted to correlate hardness Measurements with CT number. Section III documents this effort. Finally, hardness and CT correlation were investigated for a specimen taken from an actual fired nozzle. These results and the associated analysis are described in Section IV.

II. HARDNESS TEST INVESTIGATION

Efforts to discover a relatively inexpensive, yet objective procedure for measuring char depth naturally included an examination of the physical properties of the fired material. One property, hardness, was particularly appealing since it is often a reliable indicator of other material physical properties. Unfortunately, it is a destructive technique since the nozzle material must be sectioned to expose the surfaces on which the hardness will be measured. Since solid rocket motor nozzles are typically not reusable, this was not viewed as a serious deficiency. It does, however, require careful planning of the sequence of post firing analysis activities, and also places restrictions on randomization in any experimental designs.

Of interest initially was whether hardness could be measured by an available test apparatus. Another factor of interest was whether differences in human operators would influence test results. A number of methods for measuring material hardness exist. These include indentation, rebound, and scratch measurements, to mention a few [4]. A Shore Type D Durometer was made available by MFSC for pilot experiments. These experiments indicated that this apparatus had an appropriate range for carbon phenolic. It is an indentor type mechanism. Tip included angle was 30 degrees and spring force was ten pounds applied for one second. Hardness number is output via a dial indicator and can also be displayed digitally with a hard copy printout. The durometer used complies with ASTM D 2240. The pilot experiments on a sample block of carbon phenolic which had been charred in the plasma asher revealed that hardness readings were high and stable in the non heat affected (virgin) region, went through a transient in the heat affected region, and then stabilized at a noisy level in the fully charred region. The hardness response profile had the same characteristics as the CT and bulk density profiles reported in [2]. This indicated the technical feasibility for measuring char depth and the location of the char boundary. The Shore Type D Durometer was then made available by MFSC and used in all subsequent experimentation. Before each experimental run the durometer was calibrated for the test conditions (tip, pressure, and time) according to the manufacturer's published procedure.

A. Experimental Design

A designed experiment was formulated to investigate the change in hardness as a function of depth in post fired carbon phenolic. Depth was measured from a reference surface on the material, increasing in the direction from virgin material toward char. Figure 1 illustrates the measurement scheme. On any exposed surface, indentation alters the physical properties in the vicinity of the test location. It was found by trial and error that a spatial separation of 1/16 inch was adequate to minimize this effect; thus, depth measurements were made in 1/16 inch increments.

A primary factor of interest was the difference in durometer operators. Another factor was differences due to carbon phenolic manufacturer. To generate information regarding these effects, two operators were used and material satisfying the same specification on ply thickness and resin content was obtained from two different suppliers which are identified as Manufacturer 1 and

Manufacturer 2. Multiple hardness-depth profiles were generated on two different surfaces for each material sample. Because of the effect of indentation on physical properties it was not possible for both operators to take hardness readings at the same point. A separation if 1/16 inch was used. Furthermore, because of the destructive machining necessary to expose a second surface, both operators necessarily took all measurements on one surface before the second surface could be exposed. These constraints on randomization dictated a hierarchical, or nested, experimental design. The design matrix for Manufacturer 1 is shown in Figure 2. An identical matrix was applied to the sample from Manufacturer 2. Notice that on surface 1, each operator generated one profile at each

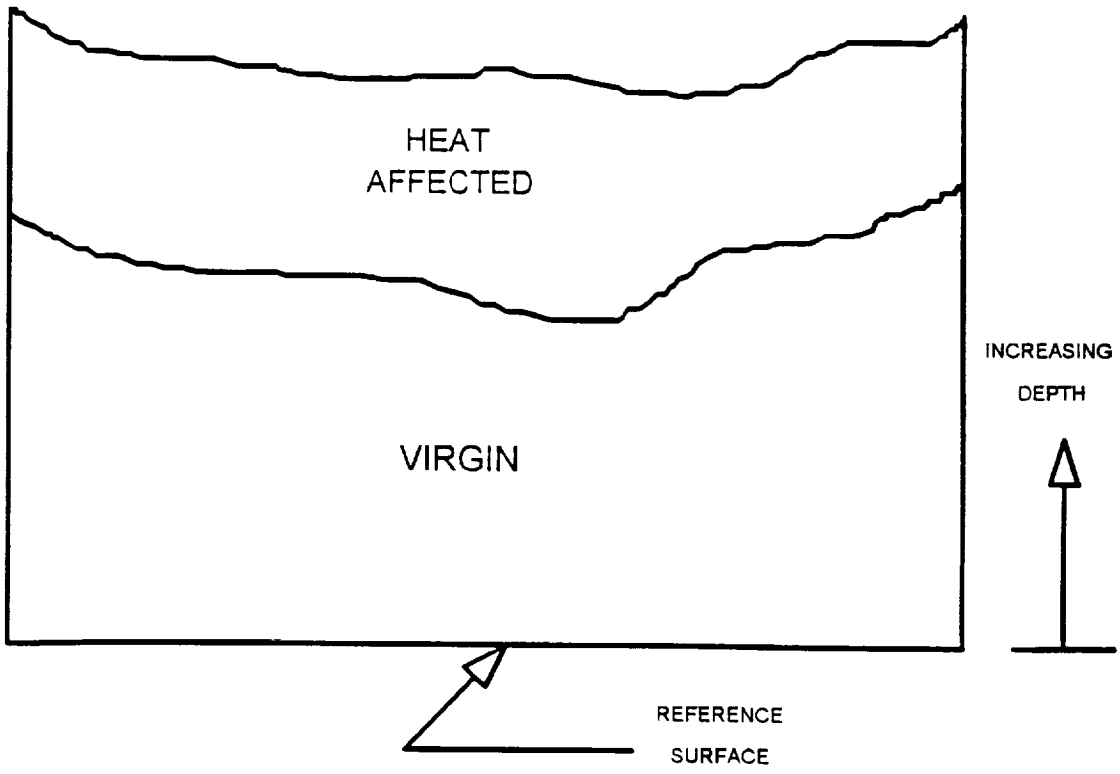

Figure 1. Depth Measurement Scheme

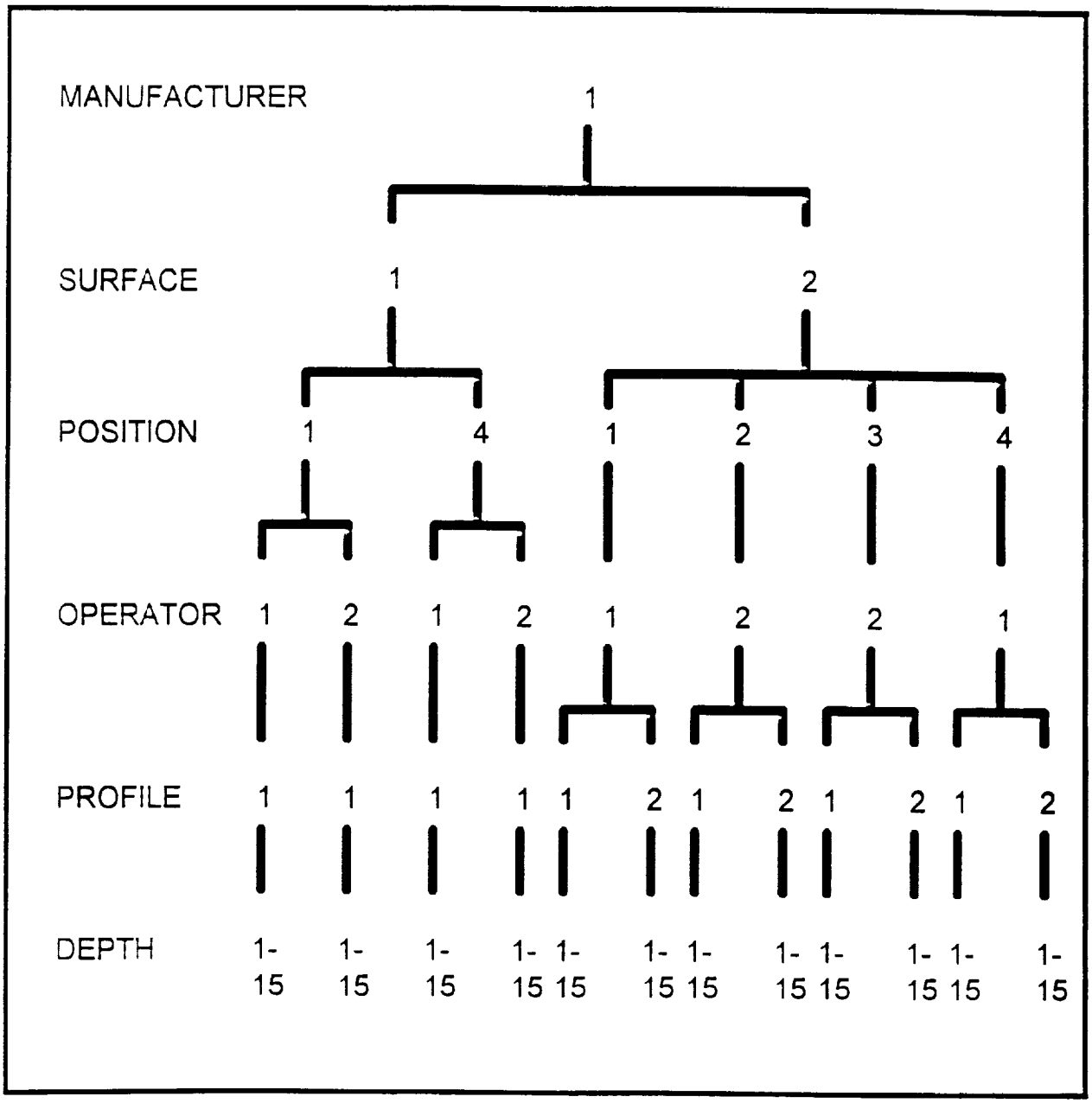

Figure 2. Nested Test Matrix For Manufacturer 1

position. At a given position, the two operator's profiles were separated by 1/16 inch. On surface 2, each operator generated two profiles at each position, the profiles being separated by 1/16 inch. This provided a mechanism for comparing within material variability and between operator variability.

One virgin material sample block, 1 X 1 X 2 inches, was used from each manufacturer. Each was charred in the plasma asher. The torch tip was placed 2 inches from the sample surface. Heat input was 1000 BTU/ft^2 sec for 20 seconds, with the flame held 90□ to the surface and directed into

the ply ends. Figure 3 shows the relative positions of the surfaces on each sample block. Surface 1 was exposed by machining 1/4 inch from a marked surface. After all measurements were made on surface 1, surface 2 was exposed by machining another 1/4 inch measured from surface 1. Figure 4 shows the relative positions of the hardness profiles on each surface.

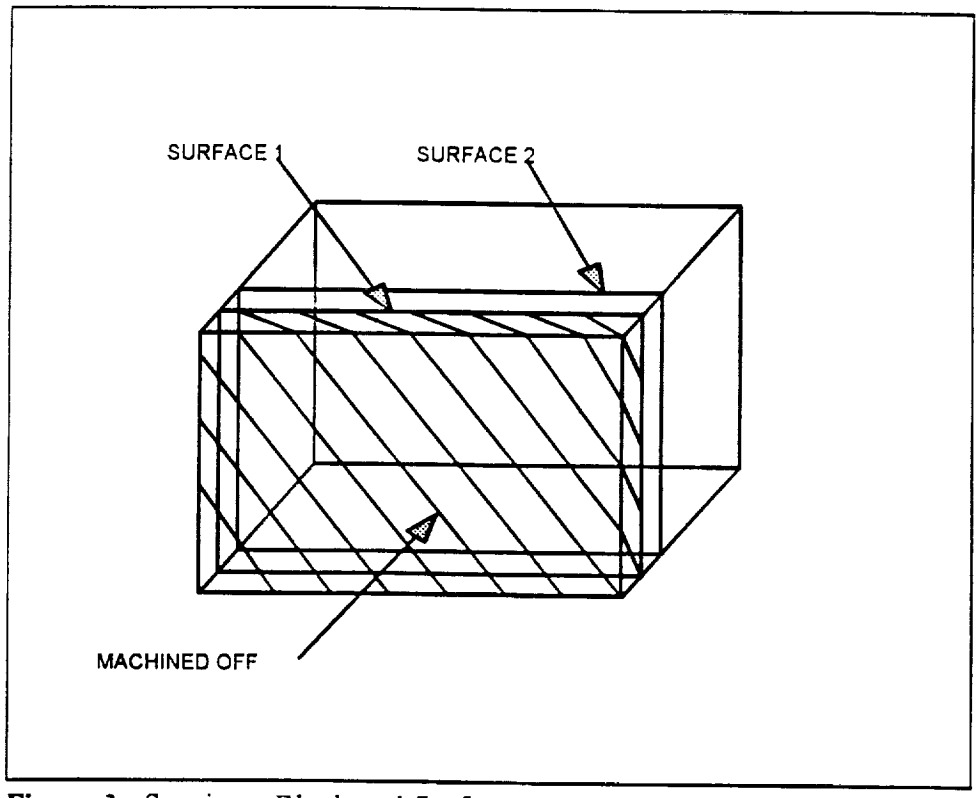

Figure 3. Specimen Block and Surfaces

B. Data and Analysis

Table 1 presents the hardness readings for Manufacturer 1, Surface 1, Position 1 for the two operators. Figure 5 shows the hardness readings as a function of depth for the data in the table. Note the relatively constant high hardness readings at low depth values, the rapid transition to low hardness values indicating the heat affected region, and the low though variable hardness readings indicating the fully charred region. Appendix A contains the raw data and associated graphs from all the hardness profiles. All of the profiles exhibit the same basic characteristics. The slope through the transition region is at least five times greater than the slope in the virgin region for all the test conditions.

The first analysis step was to examine the data for indications of special causes. The only obvious point found is shown in Figure 6. The point at depth 2 is clearly inconsistent with the trend. This anomaly is probably due to a flaw in the material caused by cracking under the plasma torch heat load .

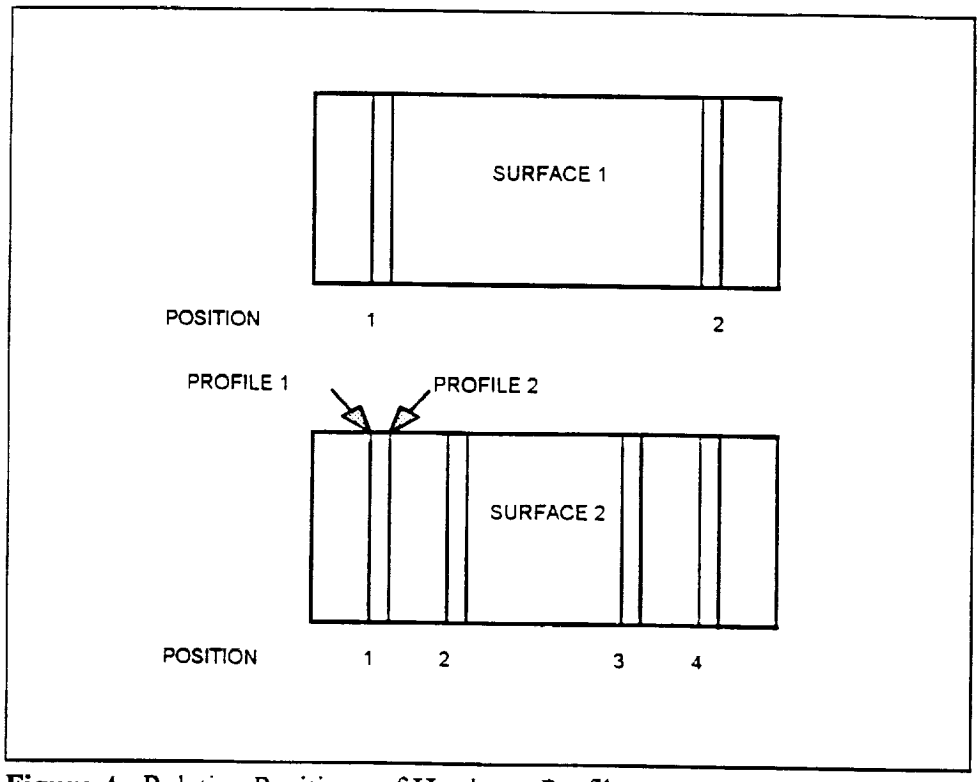

Figure 4. Relative Positions of Hardness Profiles

Since the experimental design was hierarchical, the primary tool for analysis was a dot frequency diagram which is displayed in Figure 7. Each dot in the diagram plots a durometer hardness reading. The fifteen readings for each test matrix condition are connected by a vertical line. Each of the two outer boxes enclose all of the measurements for one of the manufacturers. Within each of these manufacturer boxes are two more boxes, one for each of the surfaces.

Analysis of the dot frequency diagram was accomplished as follows. The length of the vertical lines indicates the variability in hardness at the depth points across the surface of the sample. This variability drives the heights of the boxes and is therefore the dominant source of variability. Within the manufacturer boxes, the two surfaces appear to be consistent. With the exception of the one point for Manufacturer 1, Surface 2, second profile for Operator 2, the heights of the surface boxes and their locations relative to each other are essentially the same. The manufacturer box heights and relative locations are also the same. This point was taken in the charred region, where the readings

have a great deal of variability. It also could be due to a flaw in the material caused by the plasma torch.

Table 1. Hardness Profiles. Manufacturer 1, Surface 1, Position 1

Manufacturer 1			1
Surface		1	1
Position		1	1
Operator		1	2
Profile		1	1
Depth			
1		101.8	102.0
2		101.6	101.2
3		102.2	98.7
4		101.2	99.8
5		99.2	100.1
6		99.3	99.1
7		96.6	97.6
8		97.0	96.7
9		96.7	94.8
10		90.6	89.6
11		73.2	75.7
12		67.8	68.2
13		69.9	72.1
14		73.4	80.9
15		72.1	80.0

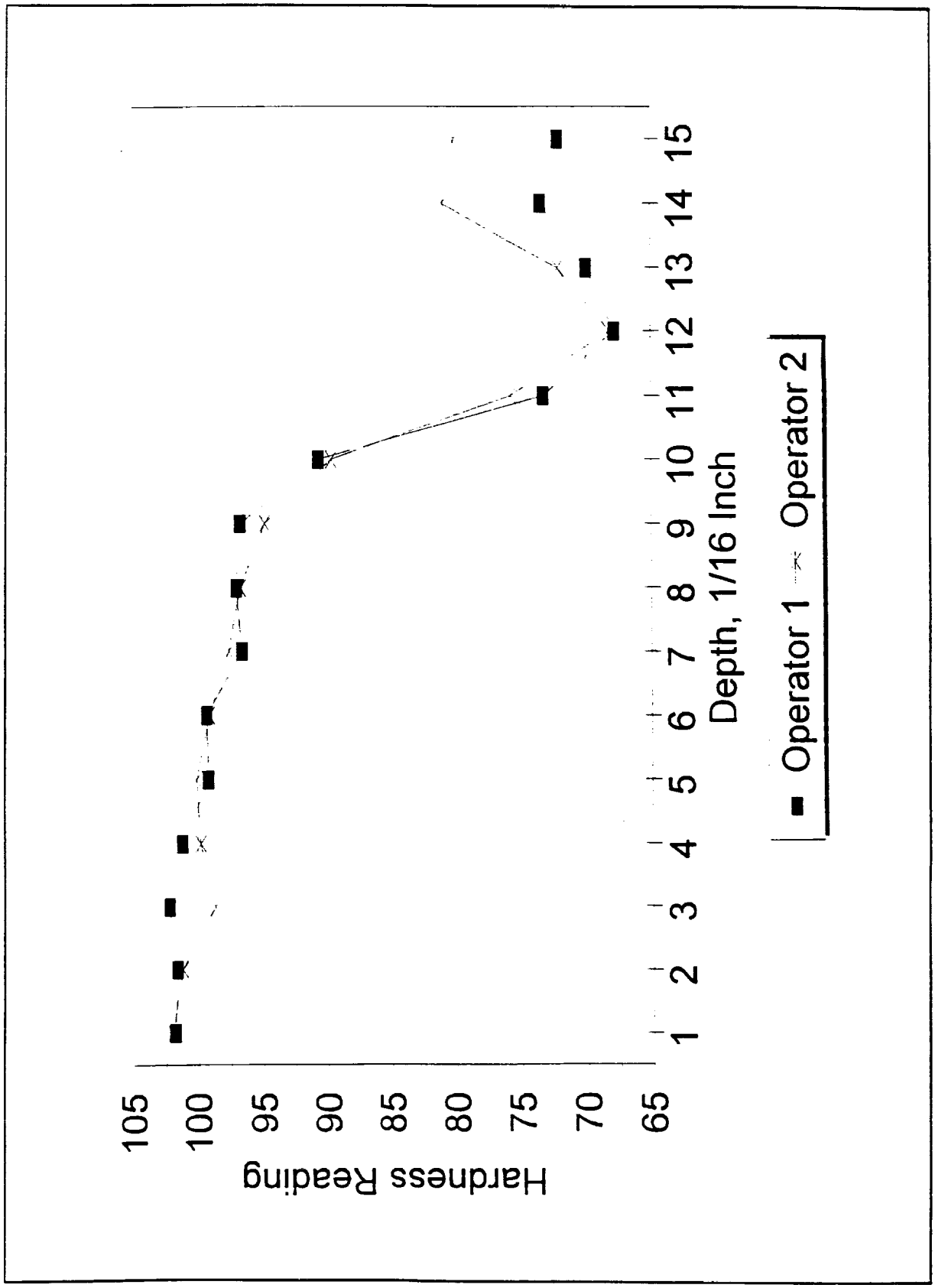

Figure 5. Hardness Profiles for Manufacturer 1, Surface 1, Position 1

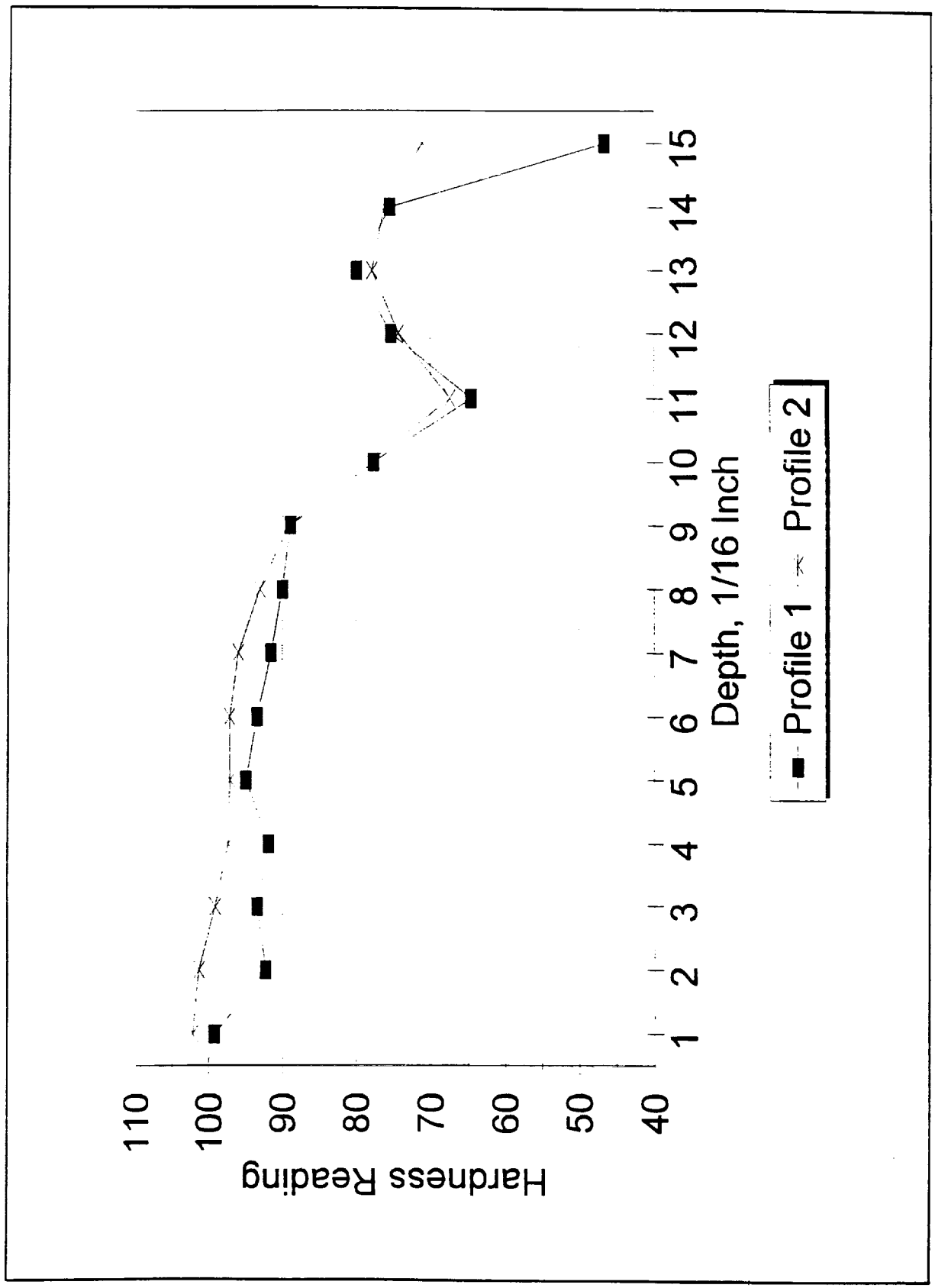

Figure 6. Hardness Profiles, Manufacturer 2, Surface 2, Position 2

For Manufacturer 1, Surface 1, Positions 1 and 2 represent readings taken in close proximity to each other by the two operators. They indicate little operator variability. Similar results are seen for the corresponding readings on the sample from Manufacturer 2. The data for Manufacturer 1, Surface 2 are readings taken in close proximity by the same operator. They capture the variability due to a combination of within operator 1 variability and material variability in a small region. From these results one can conclude that variability due to differences in operator is smaller than material/within operator variability, and that both are negligible. Furthermore, results from different material manufacturers appear essentially the same. Since most of the variability is due to depth, the relationship between depth and hardness characterizes the sample.

Additional analysis was performed on the surface one data for both manufacturers. Since the two operators measured the hardness in close proximity and at the same depth values for each position, the data constitute paired samples. A paired t test was performed for all the Surface 1 data for each manufacturer. The test did not reveal any evidence to reject the null hypothesis that the operator effect was zero in either case.

Letting $\Delta(x) = h_1(x) - h_2(x)$, where $h_i(x)$ is the hardness reading taken by operator i at depth x, control charts of $\Delta(x)$ were prepared for each Manufacturer. These are displayed in Figures 8 and 9. Depths 1 - 15 refer to Position 1 while depths 16 - 30 refer to Position 4. The purpose of these charts is to reveal any position dependent special causes. None are evident in the figures; hence it was concluded that the durometer measurement is a stable measurement system and that there is no significant operator effect.

Estimates of the char boundary were generated using the regression method described in Section I. The form of the regression relationship is $h_i(x) = b_0 + b_1x$ for each region. Figure 10 shows the results for Manufacturer 1, Surface 1, Position 1. Depths 1 - 9 were used for the virgin region and 9 - 12 for the transition region. If $h(x) = a_0 + a_1x$ is the hardness function in the virgin region and $g(x) = b_0 + b_1x$ is the hardness function in the heat affected transition region, the boundary between the two regions is given by

$$x = (b_0 - a_0)/(a_1 - b_1).$$

Table 2 shows the boundary depth for the two surfaces on the material sample from Manufacturer 1. Table 3 presents the depth for the Manufacturer 2 material. Figures 11 - 14 illustrate the relative locations.

C. Summary

The hardness investigation described above showed that the Shore Type D Durometer can be used to map the hardness profile of post fired carbon phenolic. A spacing of 1/16 inch appears to be adequate for minimizing the effects of indentation on physical properties. The durometer readings were not affected by operator or material manufacturer. Linear regression of the data in the

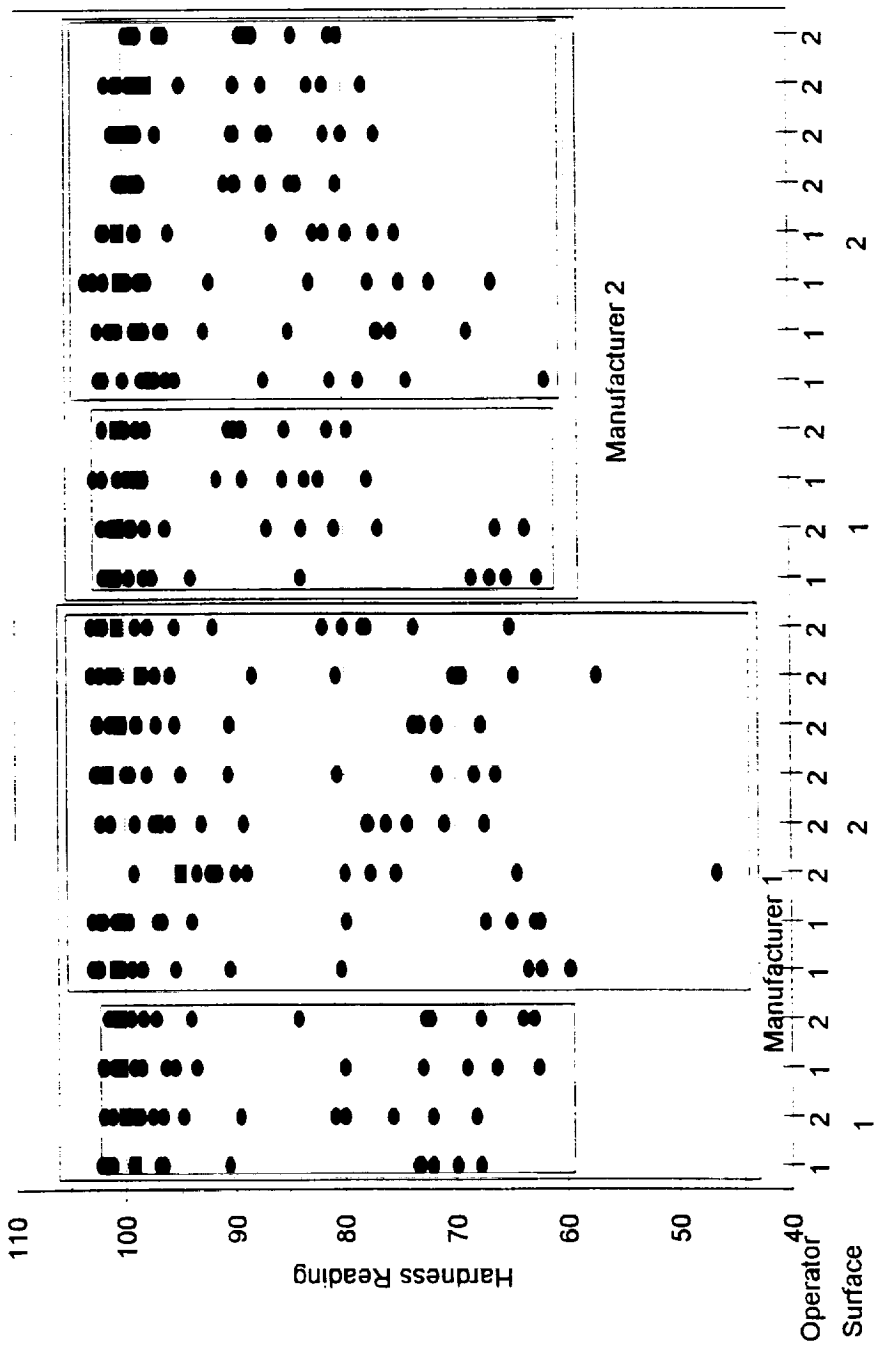

Figure 7. Dot Frequency Diagram

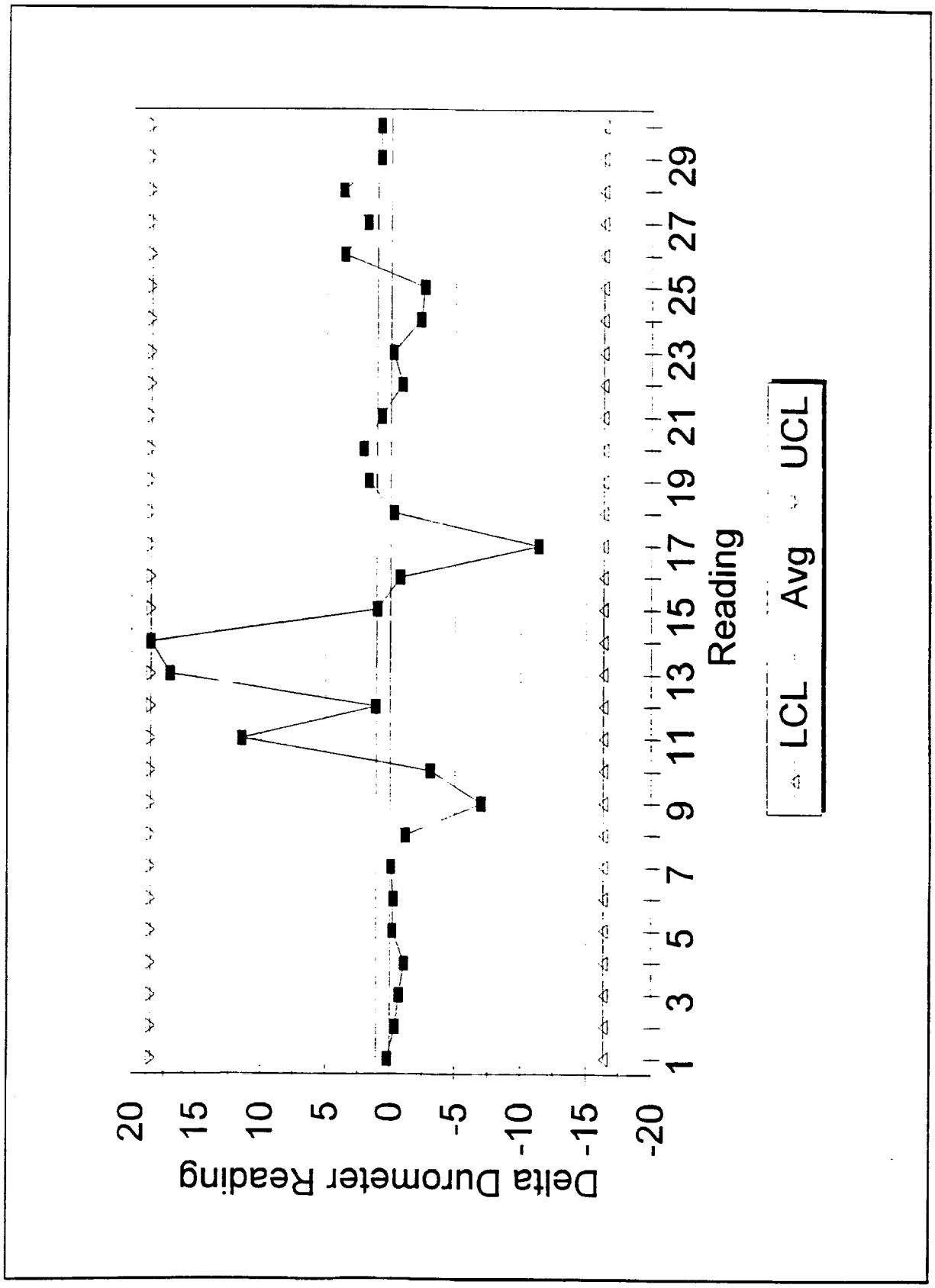

Figure 8. Delta Hardness Control Chart, Manufacturer 1

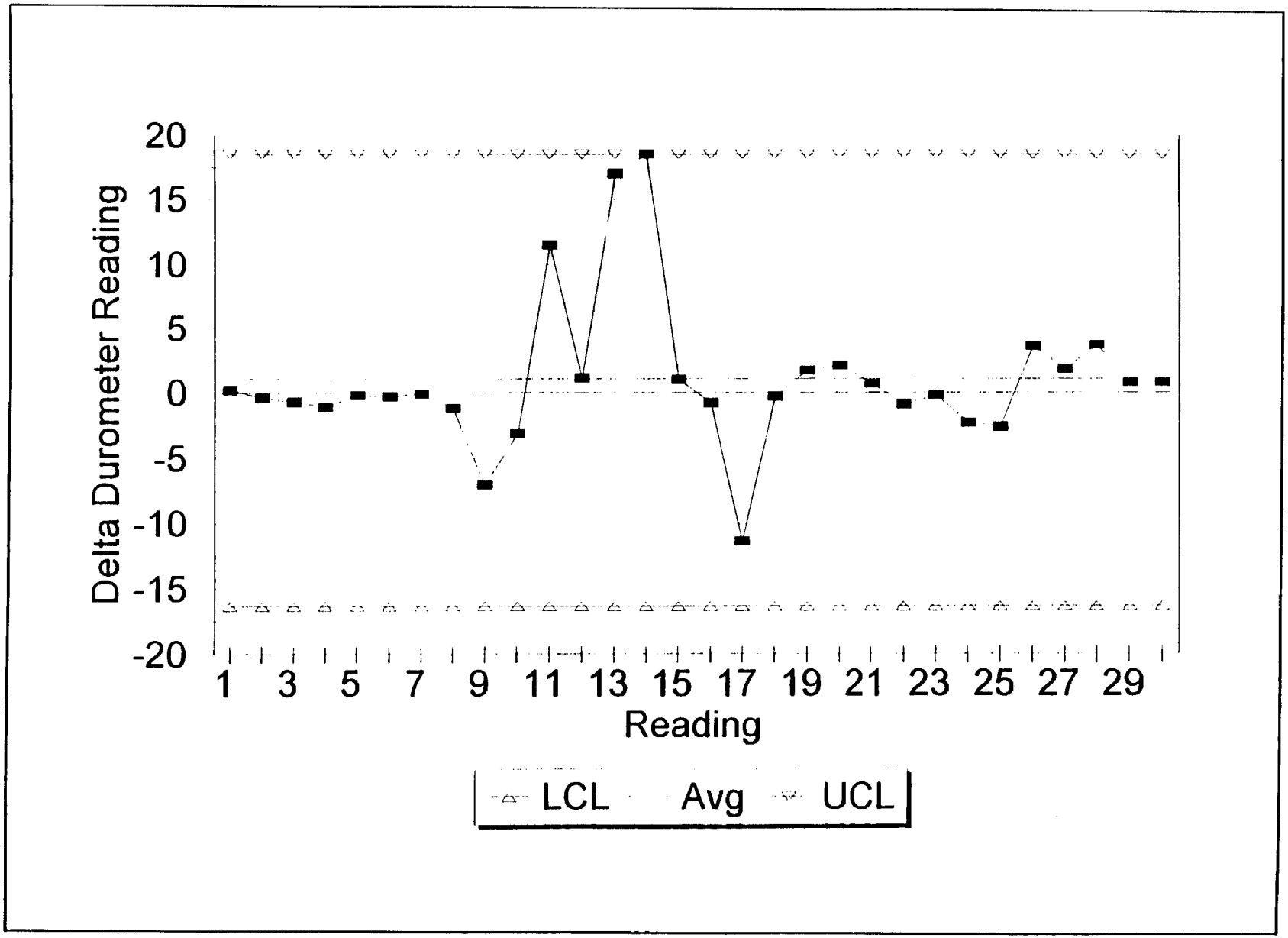

Figure 9. Delta Hardness Control Chart, Manufacturer 2

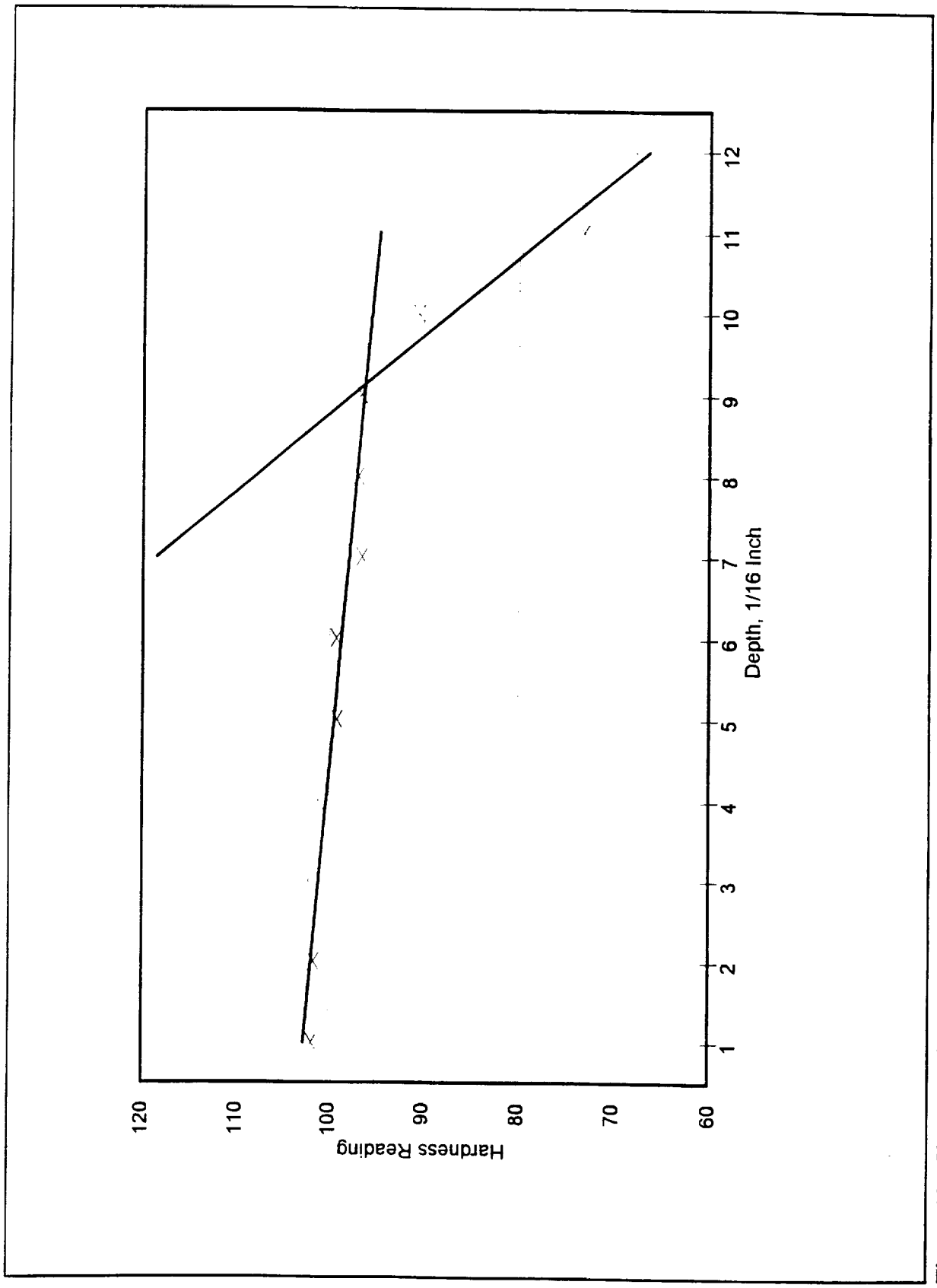

Figure 10. Char Boundary Regressions, Manufacturer 1, Surface 1, Position 1, Operator 1

Table 2. Estimated Boundary Depth, Manufacturer 1 (1/16 Inch)

Manufacturer 1				
Position	Surface 1		Surface 2	
	Location	Depth	Location	Depth
1	L1	9.14	L1	9.06
	L2	9.03	L2	9.03
2			LC1	8.97
			LC2	8.76
3			RC1	8.06
			RC2	8.02
4	R1	9.96	R1	9.18
	R2	8.80	R2	9.62

Table 3. Estimated Boundary Depth, Manufacturer 2 (1/16 Inch)

Manufacturer 2				
Position	Surface 1		Surface 2	
	Location	Depth	Location	Depth
1	L1	8.25	L1	9.87
	L2	7.81	L2	9.09
2			LC1	7.84
			LC2	7.41
3			RC1	8.25
			RC2	7.65
4	R1	8.01	R1	9.14
	R2	7.98	R2	8.33

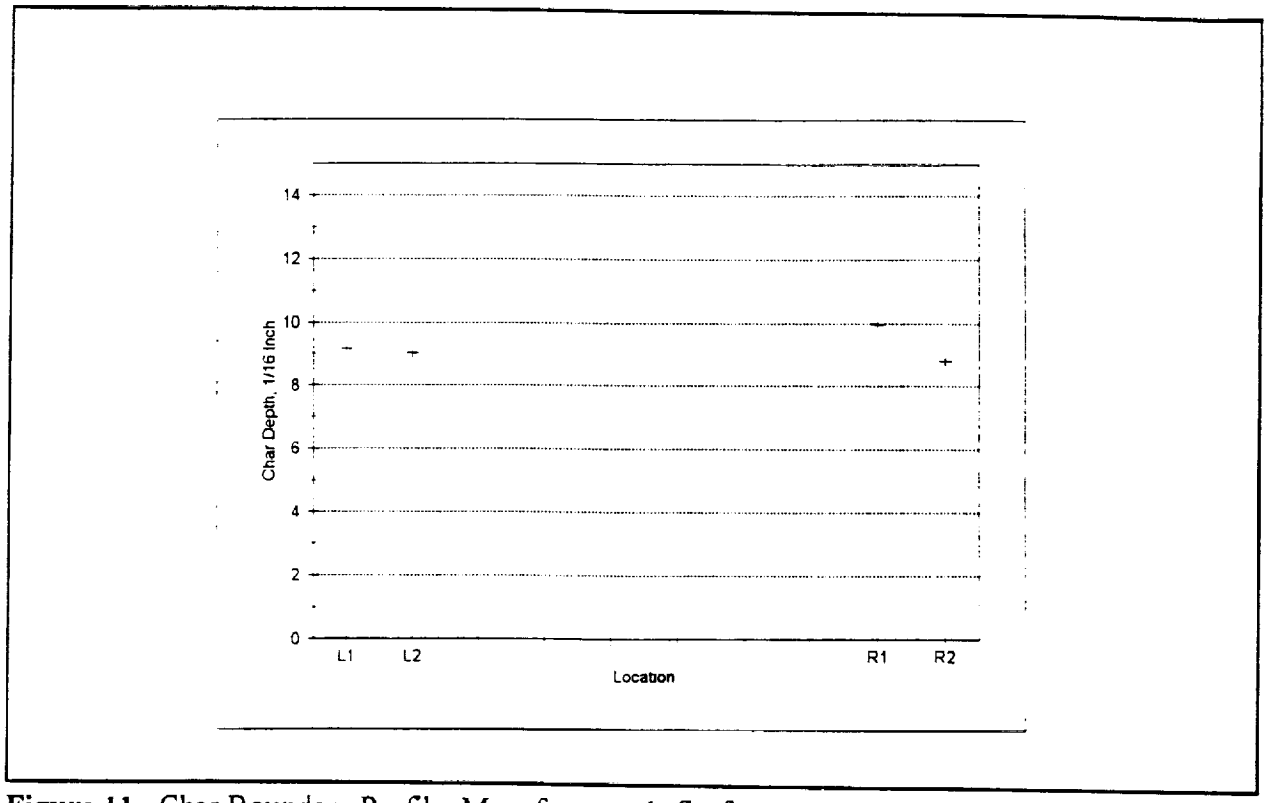

Figure 11. Char Boundary Profile, Manufacturer 1, Surface 1

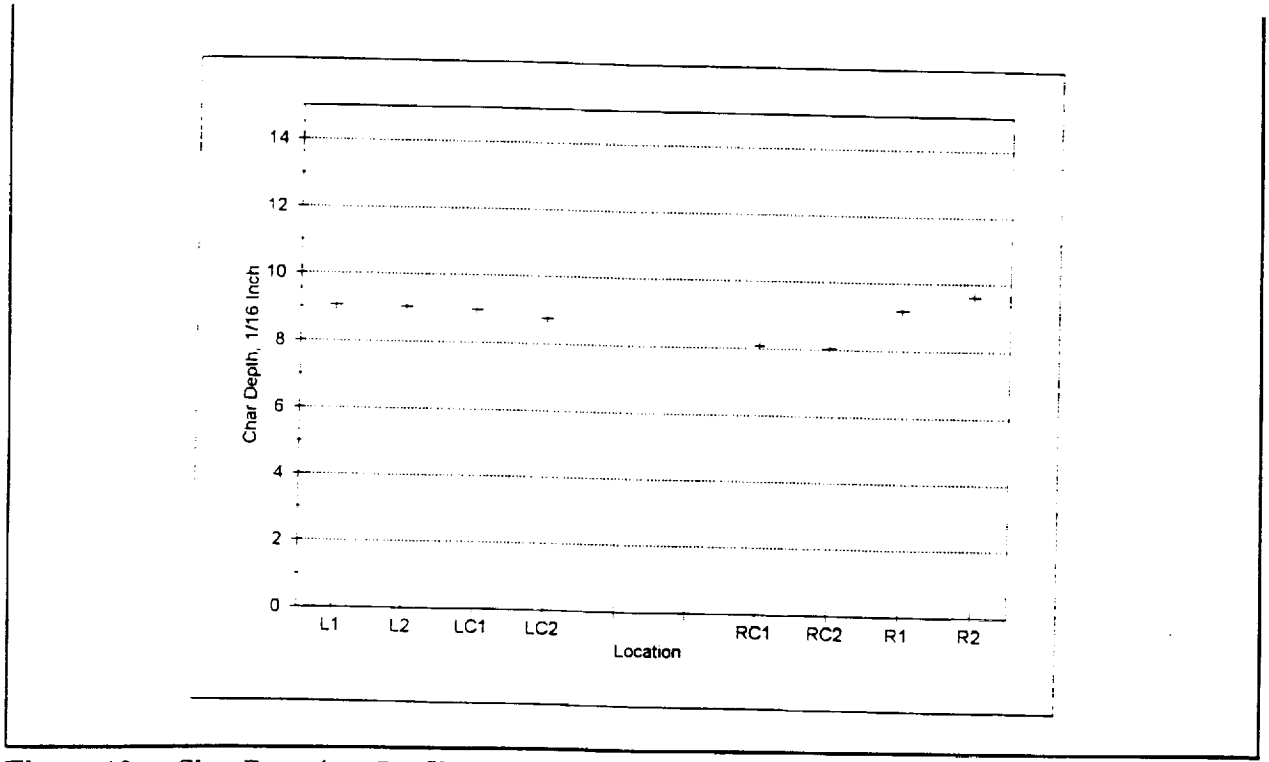

Figure 12. Char Boundary Profile, Manufacturer 1, Surface 2

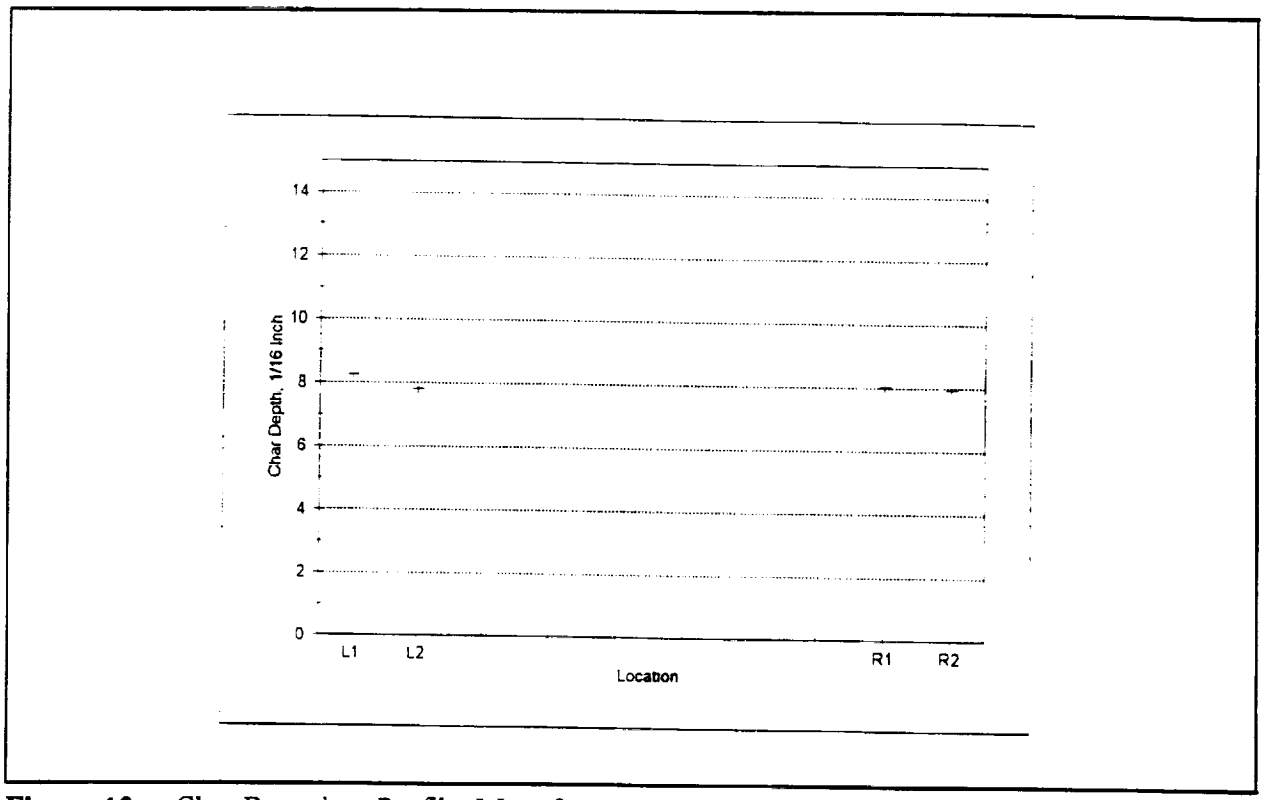

Figure 13. Char Boundary Profile, Manufacturer 2, Surface 1

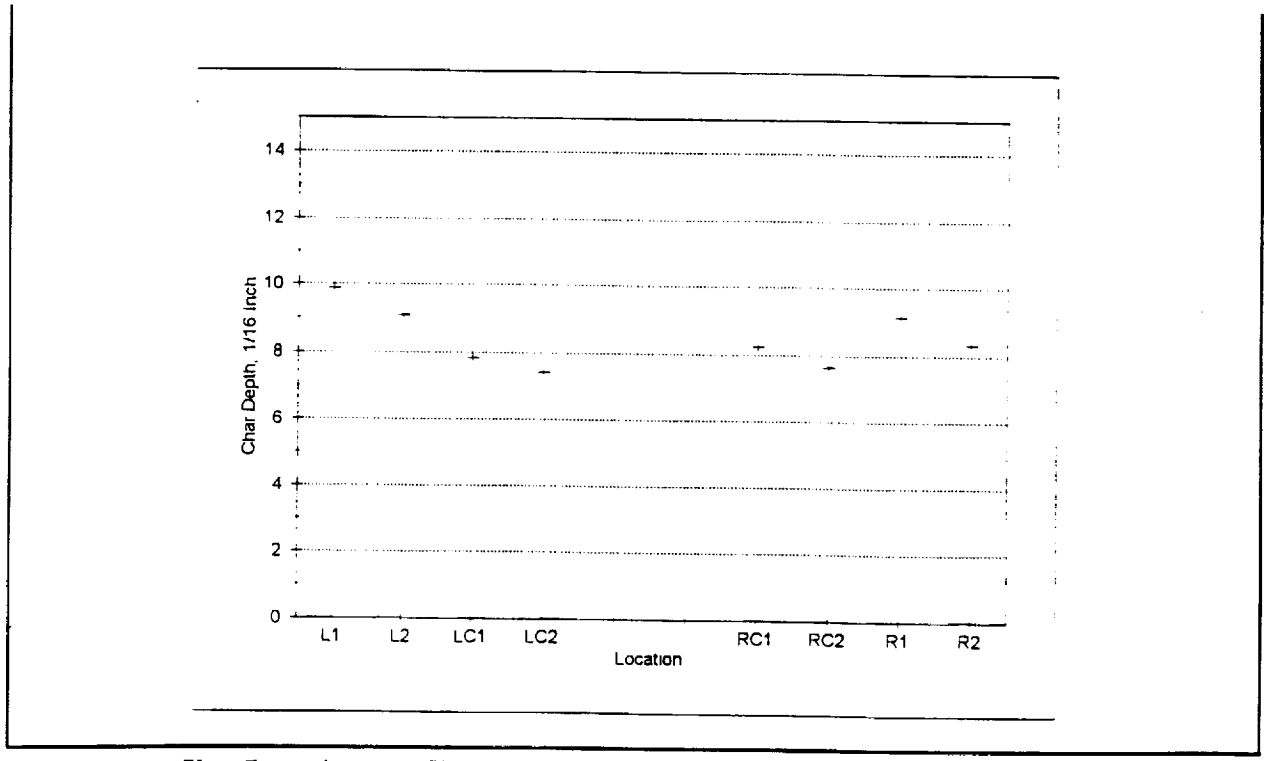

Figure 14. Char Boundary Profile, Manufacturer 2, Surface 2

virgin and transition regions can be used to estimate the location of the heat affected boundary. Additional details of the study can be found in [5].

III. COMPUTED TOMOGRAPHY - HARDNESS CORRELATION, PLASMA TORCH SAMPLES

Since char depth estimates based on the hardness measured by the Shore Type D Durometer appeared to be technically feasible, the next phase of the effort was directed toward whether these estimates were different from those obtained by computed tomography. The first investigation used the same two sample blocks from the effort described in Section II. A CT scan was made through a plane 6 mm into the sample, measured from the last surface which had been hardness tested. The scan was made by Bio-Imaging Research, Lincolnshire, Illinois, using the ACTIS+ system. MSFC arranged for this service.

The CT data were read using the Bio-Imaging work station at MSFC. Sample points corresponding to the hardness sample points 1/16 inch apart, beginning 1/32 inch from the reference surface (Figure 1) were chosen. Physical dimensions of the sample were converted into equivalent pixel lengths to locate the CT reading point. The CT number for the point was the average of a three pixel square centered at the point. After machining to expose the plane, hardness profiles were measured across the face of the sample at points corresponding to the CT points using the durometer as described in Section II. The profiles were located at 0.5, 1.0 and 1.5 inches from the right edge of the sample block. Table 4 displays the results from Manufacturer 1, Profile 1. Figure 15 is a graph of these data. Note the similarity of the two plots in the figure. All data and plots for this phase of the investigation may be found in Appendix B.

The first step in analyzing these data was to see if there was a linear relationship between CT number and hardness number. Visual analysis of CT number versus hardness number revealed that while there was evidence of a relationship there was also a large degree of scatter. A multiple linear relationship of the form

$$y_p = b_0 + b_1 x + b_2 h(x)$$

was also investigated, where y_p is predicted CT number, x is depth, and h(x) is hardness number. This relationship showed promise for predicting CT numbers, but its utility in practice is questionable since coefficients universally applicable to carbon phenolic were not investigated.

The results using the sample blocks demonstrated that the hardness profile and the corresponding CT profile across the charred carbon phenolic have similar shapes. Break points appear to occur at the same depth. This behavior suggested that both properties could be used to estimate the location of the char boundary. However, before exploring this issue, it was decided to address the question of whether these results also applied to carbon phenolic samples from actual nozzles. The next section describes this investigation.

Table 4. Manufacturer 1, Profile 1

Depth	Hardness	CT Number
1	98.9	2095.55
2	100.4	2099.55
3	102.2	2101.44
4	100.0	2102.55
5	101.3	2102.44
6	98.9	2102.88
7	99.5	2101.44
8	99.8	2100.55
9	98.6	2099.66
10	90.3	2093.66
11	78.4	2088.11
12	82.1	2085.55
13	92.3	2088.22
14	82.9	2082.66
15	84.9	2083.33

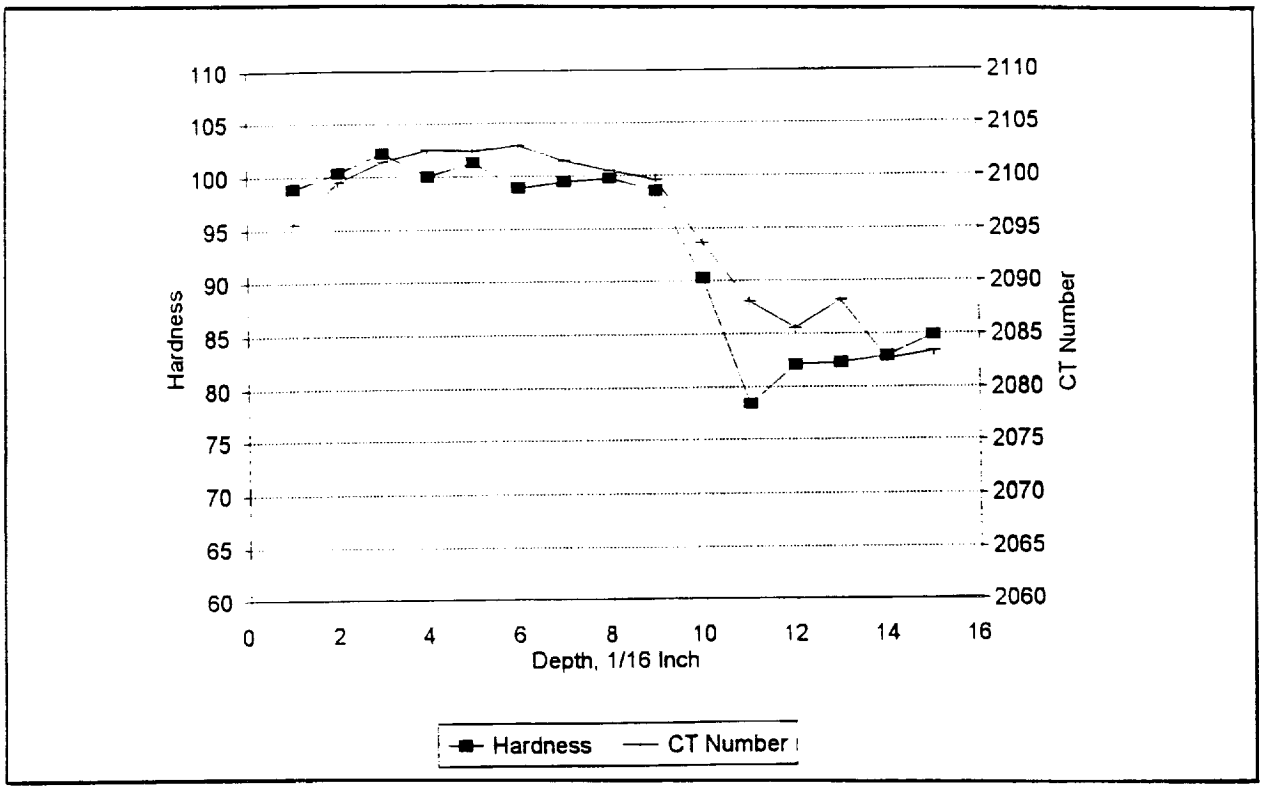

Figure 15. Sample Block Hardness and CT Number vs Depth, Manufacturer 1, Profile 1

IV. COMPUTED TOMOGRAPHY - HARDNESS CORRELATION, NOZZLE SAMPLE

To investigate the practical utility of hardness testing for estimation of char boundary location, a sample of material from a rocket nozzle which had been test fired was provided by MSFC. The carbon phenolic was identified as FM5055. The nozzle was manufactured by Thiokol, Washatch, Utah, using NARC rayon produced by British Petroleum Chemicals. Figure 16 is a typical cross section of the sample. The test firing was conducted on November 1, 1991, as part of the Solid Propulsion Integrity Program 2. The motor was a modified NASA solid rocket Insulation Test Motor. The Propellant was HTPB and firing time was 60 seconds.

The nozzle sample was scanned using the ACTIS+ system through three planes spaced 10 mm apart. After scanning the sample was cut using a diamond saw to expose the surfaces corresponding to the planes. The surfaces were identified as Surface 2 through Surface 4. Five profiles were mapped across each surface. Figure 17 shows the map locations. Map 1 was located 1/4 inch from the right edge of the silica phenolic with the rest of the maps spaced 1/2 inch apart. Map 1 on surface 4 was remeasured 3/8 inch from the edge after the sample was chipped during hardness testing. Procedures for estimating CT number and measuring hardness were identical to those described above. Measurement points were space at 1/16 inch intervals, beginning 1/16 inch into the virgin carbon phenolic measured from the silica phenolic interface. Table 5 shows the data for Surface 2, Map 2. Figure 18 plots the data. All nozzle data and associated plots can be found in Appendix C.

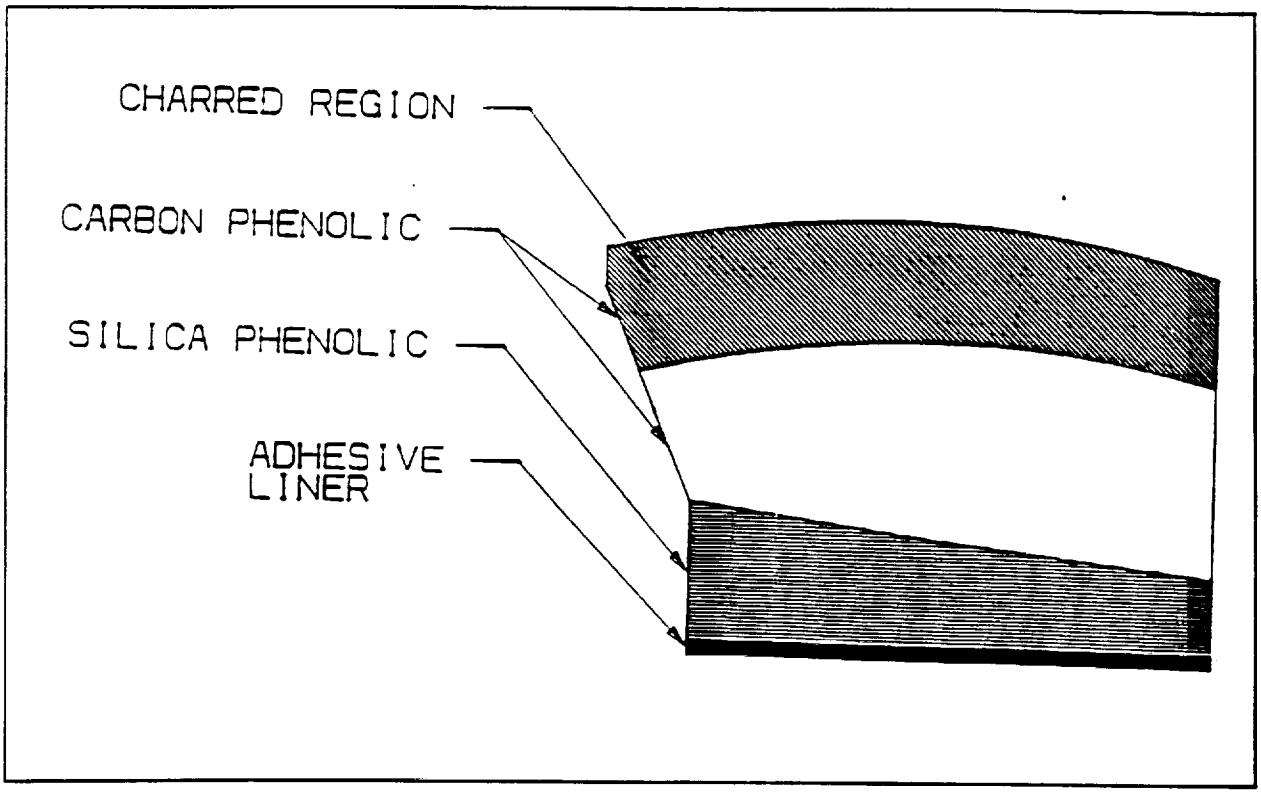

Figure 16. Nozzle Sample Cross Section

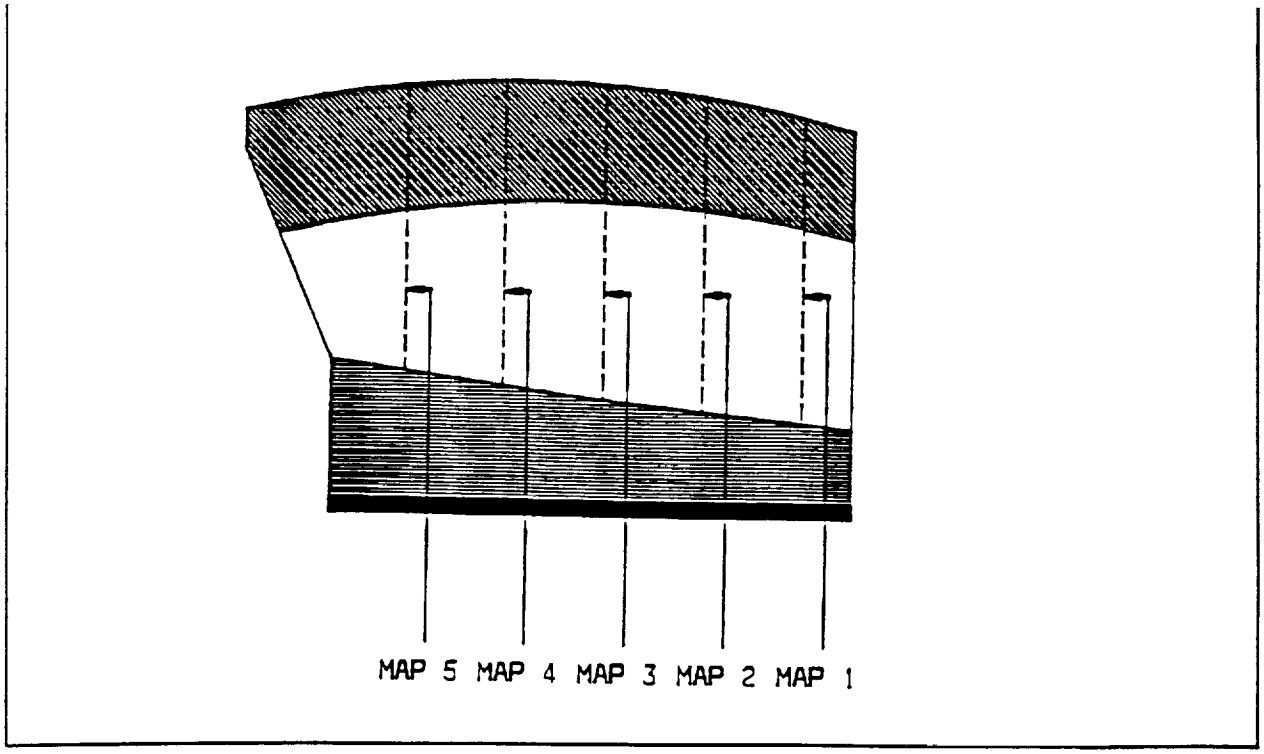

Figure 17. Nozzle Sample Map Locations

Table 5. Nozzle Sample Hardness and CT Number, Surface 2, Map 2

Position	Hardness	CT Number
1	94.6	2069.67
2	94.3	2068.78
3	93.3	2066.44
4	93.5	2068.44
5	92.9	2068.11
6	87.9	2068.11
7	88.7	2066.56
8	87.8	2066.67
9	91	2065.33
10	89.6	2066.67
11	86.9	2064.67
12	87.2	2064.67
13	84.3	2064.67
14	82.4	2065.33
15	76.6	2062.00
16	61.3	2059.67
17	59.3	2055.89
18	62.8	2053.78
19	62.5	2052.00

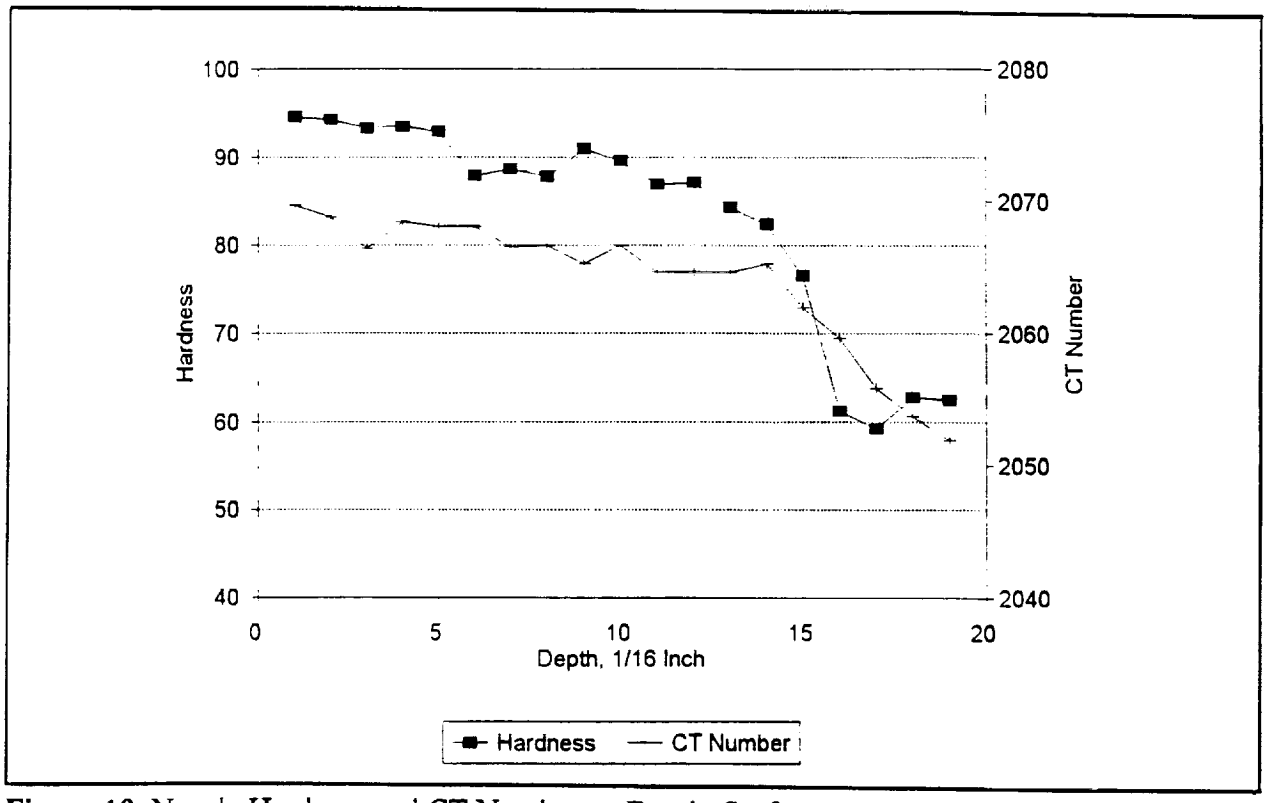

Figure 18. Nozzle Hardness and CT Number vs Depth, Surface 2, Map 2

As with the sample blocks, the relationship between CT number and hardness was explored. Figure 18 indicates that both characteristics have the same basic shape as a function of location. Figure 19 is a scatter plot of all nozzle sample CT numbers versus hardness numbers. The scatter is somewhat improved over that obtained with the sample blocks, but is still too great for practical linear estimation. Multiple linear regression still looked promising, but requires more detailed experimentation to define its practical utility.

The remainder of the investigation concentrated on the equivalence of CT and hardness estimates of char boundary location. For each map, the boundary position was estimated using CT numbers and hardness numbers. Visual interpretation of the graphs was used to determine the points for each regression relationship. Tables 7 and 8 portray the results. As can be seen, they are very close. The largest difference is 1.9/16, or approximately 0.12 inch.

Since the results of the depth comparisons constitute matched pairs, their equivalence was subjected to a hypothesis test. The Wilcoxin matched pairs test [6, pp 280-283] was used for this purpose to avoid assumptions regarding the distribution of the difference and also since the sample size was small (15). The test could not reject the null hypothesis of equivalence at 0.05 significance. It was therefore concluded that hardness measured using the Shore Type D Durometer can be used to estimate the location of the char boundary in carbon phenolic material to an accuracy equivalent to that obtained using computed tomography.

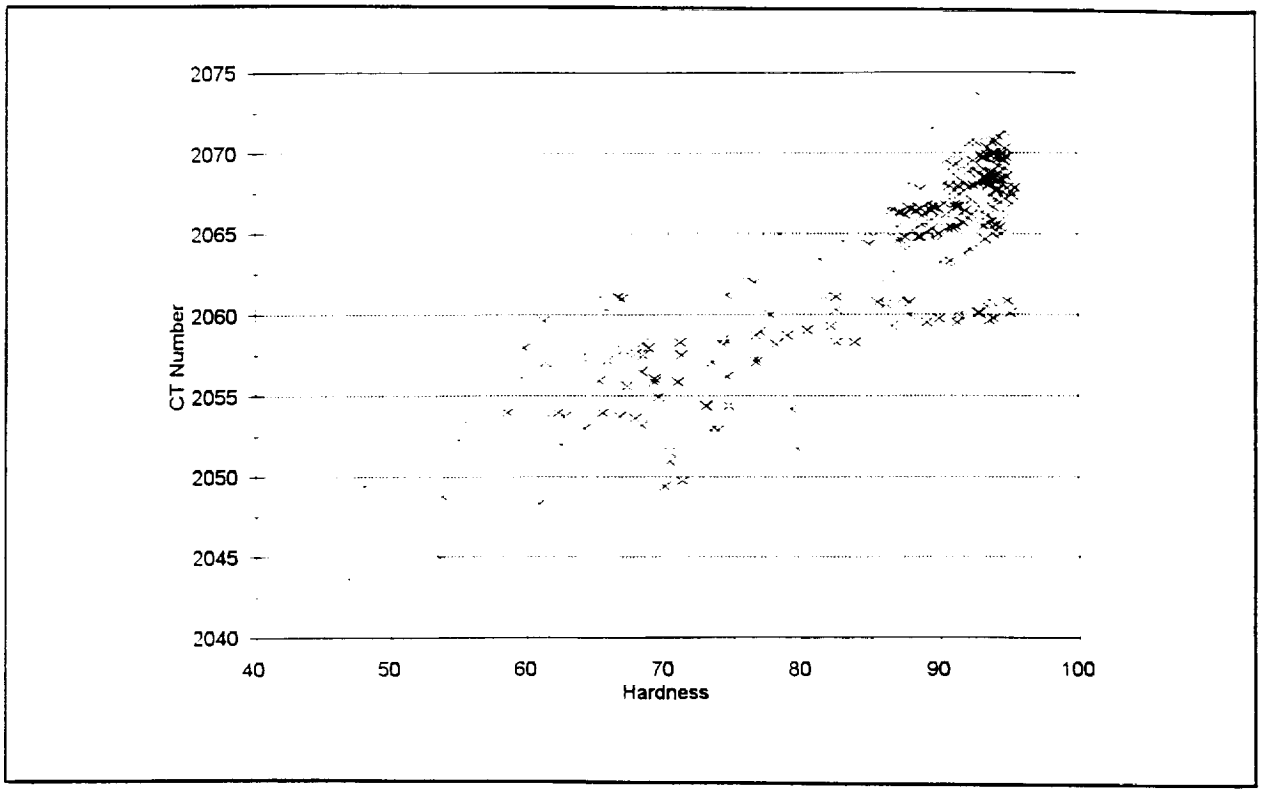

Figure 19 Nozzle Sample CT - Hardness Scatter Plot

Table 6. Hardness Predicted Char Depth

Surface	Map	Virgin Points	Transition Points	Depth
2	1	8-12	12-16	12.4
	2	6-12	12-16	12.4
	3	2-14	14-16	13.8
	4	9-12	12-15	12.2
	5	5-10	10-13	10.1
3	1	9-14	14-16	14.2
	2	9-14	14-17	14.1
	3	10-14	14-16	14.0
	4	8-13	13-15	12.9
	5	4-11	11-13	10.8
4	1	5-15	15-17	14.9
	2	6-14	14-17	14.2
	3	9-15	15-17	14.6
	4	4-12	12-15	12.4
	5	7-11	11-13	11.1

Table 7. Computed Tomography Predicted Char Depth

Surface	Map	Virgin Points	Transition Points	Depth
2	1	9-13	13-16	13.1
	2	4-14	14-19	14.3
	3	4-13	13-15	13.1
	4	2-11	11-16	11.6
	5	6-11	11-12	11.0
3	1	6-14	14-17	14.3
	2	9-15	15-18	15.1
	3	4-14	14-19	14.5
	4	6-13	13-18	13.1
	5	1-10	10-16	10.1
4	1	7-13	13-19	13.1
	2	6-13	13-17	13.3
	3	14-15	15-16	15.0
	4	8-12	12-18	11.8
	5	6-9	9-17	10.4

V. CONCLUSIONS AND RECOMMENDATIONS

This investigation demonstrated the technical feasibility of using hardness testing to estimate the location of the boundary between virgin and heat affected regions in carbon phenolic nozzle material. Operator and material source have no significant impact on the variability of the hardness readings; i.e., these components of hardness variance are negligible. Similar profile shapes were found for both hardness and computed tomography measurements in mechanically fired sample blocks and in actually test fired nozzle material. No statistically significant difference was found in location estimates made using CT and hardness for actual carbon phenolic nozzle material. It is therefore concluded that the less expensive hardness method can be used for this purpose.

A multiple linear relationship between hardness and CT number appears to exist. Additional experimentation is recommended to characterize this correlation for carbon phenolic and other materials.

REFERENCES

1. Hoover, C. B., **Density Gradient of Ablated Carbon Phenolic Slice From Motor 1A**, Southern Research Institute Report SRI-MME-92-64-6672.3, January, 1992

2. Northrup, M., **Using Computed Tomography to Determine Char Depth**, Hercules Aerospace, Undated Report

3. Ikeda, H., Y. Yamamoto and M. Kohno, *A Study of Erosion and Ablation Mechanisms in Solid Rocket Exit Cone*, **Proceedings of the Sixteenth International Symposium on Space Technology and Science**, Sapporo, 1988, Vol. I, AGNE Publishing, 1988

4. Boyer, H., ed, **Hardness Testing**, ASM International, 1987

5. Schad, K. C., **Durometer Hardness Testing for Char Measurement of Post-Fire Carbon Phenolic**, Thesis, The University of Alabama in Huntsville, 1992

6. Conover, W. J., **Practical Nonparametric Statistics**, 2nd Edition, John Wiley and Sons, New York, NY, 1980

APPENDIX A

Manufacturer	1	1
Surface	1	1
Position	1	1
Operator	1	2
Profile	1	1

Depth		
1	101.8	102.0
2	101.6	101.2
3	102.2	98.7
4	101.2	99.8
5	99.2	100.1
6	99.3	99.1
7	96.6	97.6
8	97.0	96.7
9	96.7	94.8
10	90.6	89.6
11	73.2	75.7
12	67.8	68.2
13	69.9	72.1
14	73.4	80.9
15	72.1	80.0

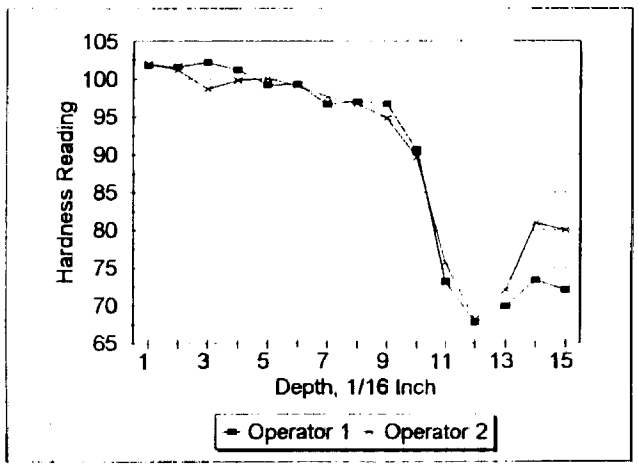

Manufacturer	1	1
Surface	1	1
Position	4	4
Operator	1	2
Profile	1	1

Depth		
1	101.9	101.5
2	102.1	101.6
3	101.1	101.5
4	101.1	101.0
5	100.4	100.5
6	99.2	99.5
7	98.6	98.4
8	96.4	97.3
9	95.6	94.1
10	93.6	84.2
11	80.0	72.3
12	69.0	63.0
13	66.4	67.8
14	73.0	72.8
15	62.6	64.0

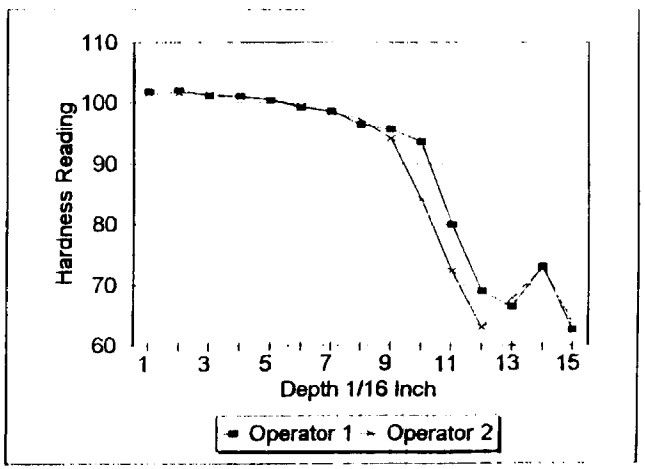

Manufacturer	1	1
Surface	2	2
Position	1	1
Operator	2	2
Profile	1	2
Depth		
1	102.5	102.5
2	102.7	102.4
3	102.4	101.3
4	102.7	100.3
5	101.6	100.4
6	99.9	98.9
7	99.5	99.0
8	98.0	97.2
9	95.0	95.5
10	90.6	90.5
11	80.6	71.6
12	66.4	67.7
13	66.4	73.7
14	71.6	73.1
15	68.3	73.8

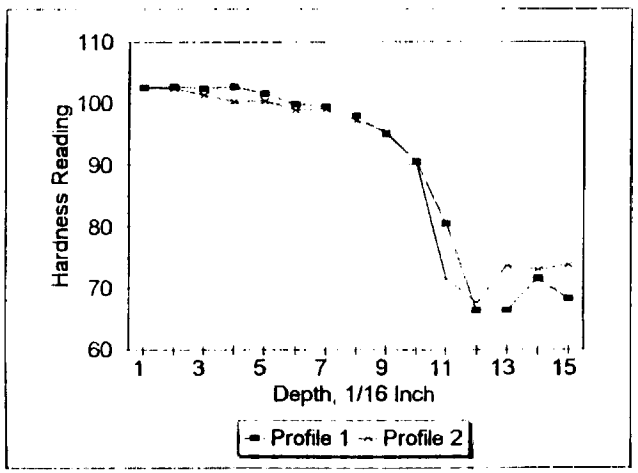

Manufacturer	1	1
Surface	2	2
Position	2	2
Operator	2	2
Profile	1	2
Depth		
1	99.2	102.2
2	92.3	101.3
3	93.5	99.1
4	91.9	97.4
5	95.0	97.1
6	93.5	97.2
7	91.6	96.0
8	90.0	93.1
9	88.9	89.2
10	77.6	78.0
11	64.5	67.4
12	75.3	74.3
13	79.9	77.8
14	75.4	76.2
15	46.6	71.0

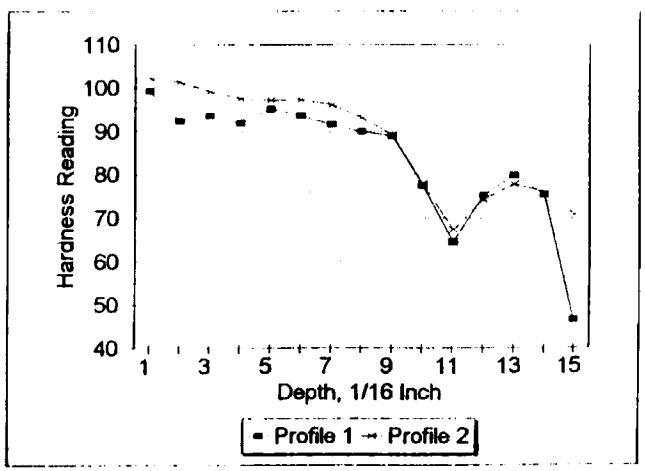

Manufacturer	1	1
Surface	2	2
Position	3	3
Operator	2	2
Profile	1	2
Depth		
1	102.2	103.0
2	103.0	102.3
3	101.3	102.3
4	100.7	101.9
5	98.6	100.7
6	98.3	99.0
7	97.3	97.9
8	95.9	95.5
9	88.4	92.0
10	80.7	80.1
11	69.4	73.7
12	69.7	77.9
13	70.2	81.9
14	64.7	78.3
15	57.3	65.1

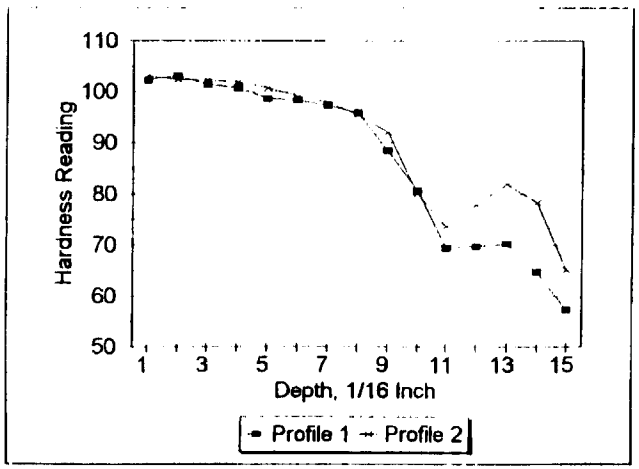

Manufacturer	1	1
Surface	2	2
Position	4	4
Operator	1	1
Profile	1	2
Depth		
1	103.0	102.3
2	102.6	102.0
3	102.3	103.0
4	102.4	100.8
5	100.9	100.5
6	100.3	100.4
7	99.4	99.7
8	98.5	96.7
9	95.5	97.1
10	90.5	94.0
11	80.3	79.8
12	59.7	67.3
13	59.8	62.4
14	63.5	62.9
15	62.3	65.0

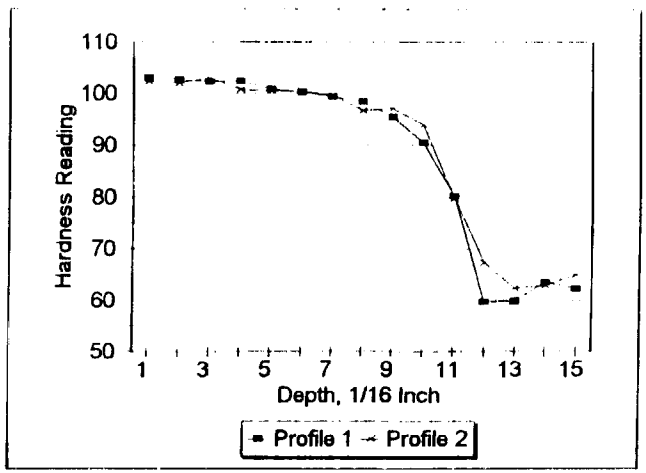

Manufacturer	2	2
Surface	1	1
Position	1	1
Operator	1	2
Profile	1	1
Depth		
1	101.8	102.0
2	101.3	100.9
3	101.9	101.2
4	100.6	99.5
5	100.8	100.6
6	99.5	99.2
7	98.2	98.1
8	97.5	96.3
9	94.0	87.0
10	83.9	80.8
11	65.3	76.8
12	62.6	63.7
13	66.8	83.8
14	68.5	87.0
15	65.3	66.3

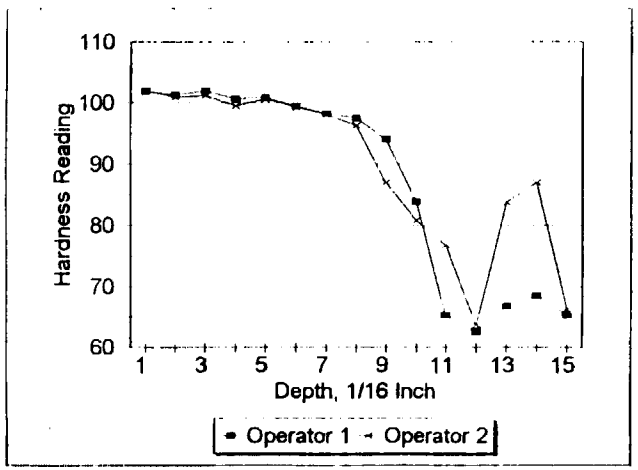

Manufacturer	2	2
Surface	1	1
Position	4	4
Operator	1	2
Profile	1	1
Depth		
1	102.7	101.9
2	101.9	
3	100.5	100.2
4	98.8	100.5
5	98.5	100.6
6	99.1	99.8
7	99.7	98.8
8	98.2	98.0
9	91.6	89.3
10	82.2	79.6
11	77.8	81.4
12	83.5	85.3
13	85.5	89.2
14	89.2	90.0
15	89.2	90.0

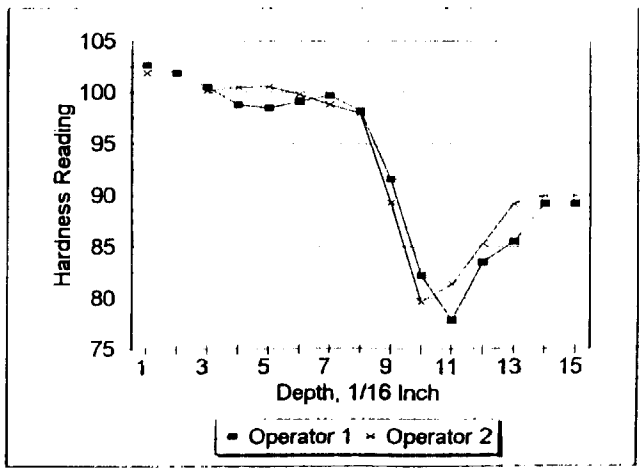

Manufacturer	2	2
Surface	2	2
Position	1	1
Operator	1	1
Profile	1	2
Depth		
1	101.7	102.3
2	102.2	101.2
3	100.0	101.1
4	100.0	100.5
5	97.9	98.7
6	97.2	96.4
7	98.3	99.0
8	96.1	98.1
9	97.1	96.7
10	95.3	92.7
11	81.1	76.7
12	74.2	75.5
13	78.5	76.9
14	87.2	84.9
15	61.8	68.8

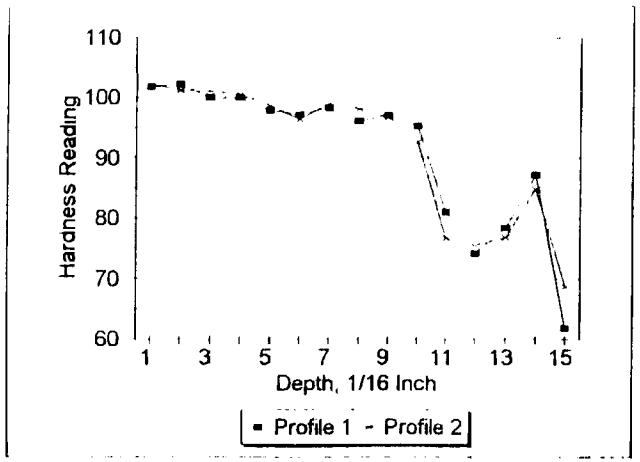

Manufacturer	2	2
Surface	2	2
Position	2	2
Operator	2	2
Profile	1	2
Depth		
1	100.4	100.9
2	99.8	101.0
3	99.7	100.0
4	100.1	100.4
5	98.8	99.2
6	99.9	98.7
7	98.5	99.4
8	98.8	97.0
9	90.8	90.2
10	84.1	80.0
11	80.5	81.6
12	84.7	86.7
13	89.9	89.8
14	89.7	87.3
15	87.3	77.0

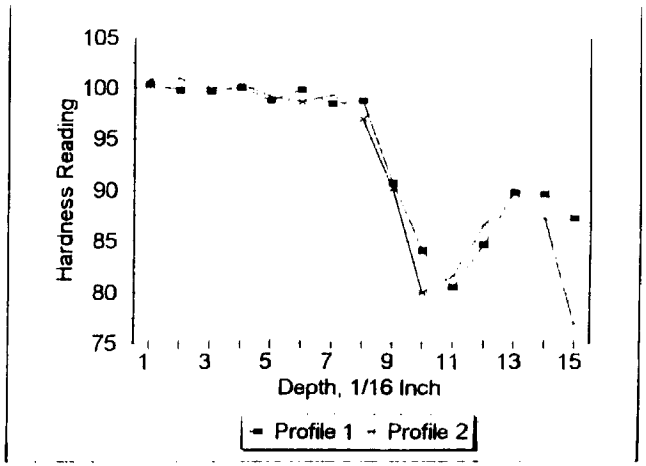

Manufacturer	2	2
Surface	2	2
Position	3	3
Operator	2	2
Profile	1	2

Depth		
1	100.3	99.3
2	101.6	96.3
3	100.7	96.8
4	98.9	99.7
5	97.8	99.0
6	99.4	98.7
7	97.8	99.0
8	98.4	99.6
9	94.8	88.9
10	83.1	80.3
11	78.1	81.1
12	81.7	84.5
13	87.3	88.5
14	89.8	89.4
15	90.0	88.1

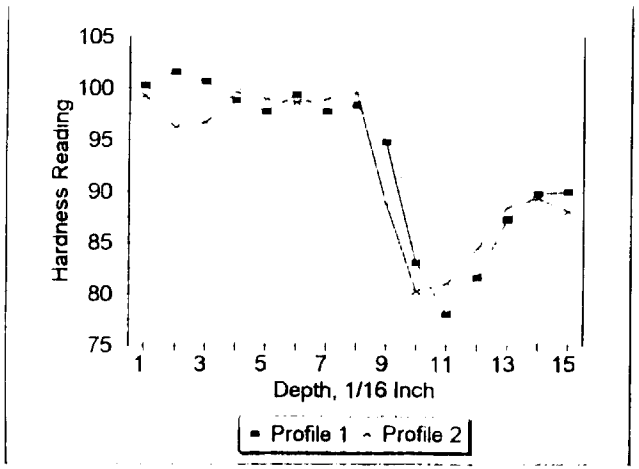

Manufacturer	2	2
Surface	2	2
Position	4	4
Operator	1	1
Profile	1	2

Depth		
1	102.6	101.7
2	103.4	101.6
3	102.7	101.9
4	101.7	101.6
5	100.3	100.4
6	98.6	98.8
7	97.9	99.0
8	99.6	98.9
9	98.4	95.9
10	92.2	86.4
11	77.6	75.2
12	72.1	77.1
13	74.8	82.6
14	83.0	81.6
15	66.6	79.6

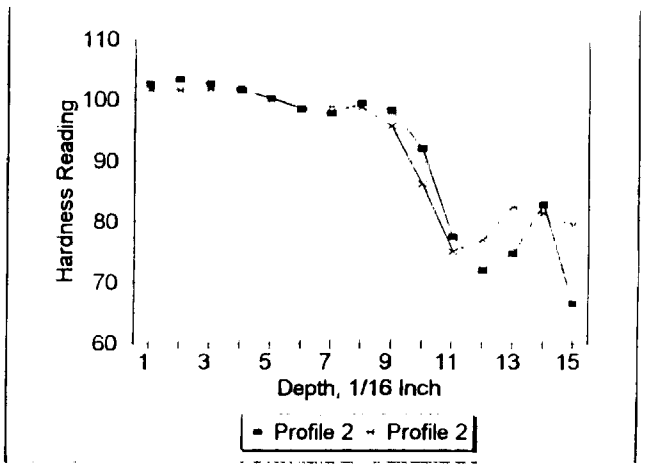

APPENDIX B

Sample	1
Position	1

Depth	Hard	CT
1	98.9	2095.55
2	100.4	2099.55
3	102.2	2101.44
4	100.0	2102.55
5	101.3	2102.44
6	98.9	2102.88
7	99.5	2101.44
8	99.8	2100.55
9	98.6	2099.66
10	90.3	2093.66
11	78.4	2088.11
12	82.1	2085.55
13	82.3	2088.22
14	82.9	2082.66
15	84.9	2083.33

Sample	1
Position	2

Depth	Hard	CT
1	94.7	2099.22
2	98.1	2101.33
3	98.5	2100.77
4	98.0	2103.88
5	97.6	2103.77
6	98.4	2105.22
7	97.1	2104.66
8	90.1	2102.88
9	90.0	2095.00
10	79.1	2092.11
11	71.6	2088.66
12	78.1	2094.00
13	71.4	2090.66
14	70.3	2089.00
15	63.3	2088.11

Sample	1
Position	3

Depth	Hard	CT
1	102.1	2102.11
2	101.8	2103.44
3	101.6	2100.55
4	99.7	2101.33
5	99.4	2101.66
6	98.9	2100.20
7	99.0	2103.33
8	98.2	2099.00
9	98.0	2100.00
10	92.6	2096.88
11	74.1	2091.88
12	66.7	2088.22
13	68.4	2087.44
14	67.2	2087.33
15	66.1	2087.77

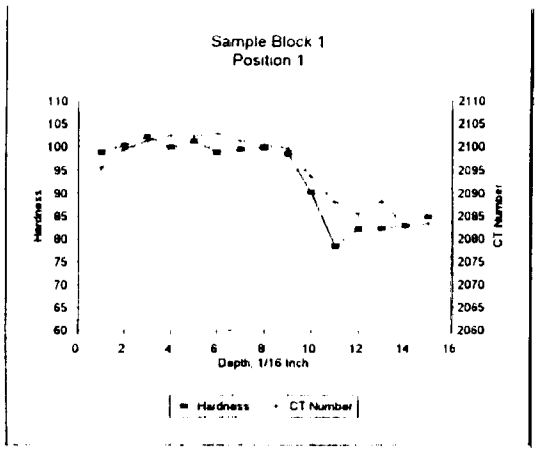

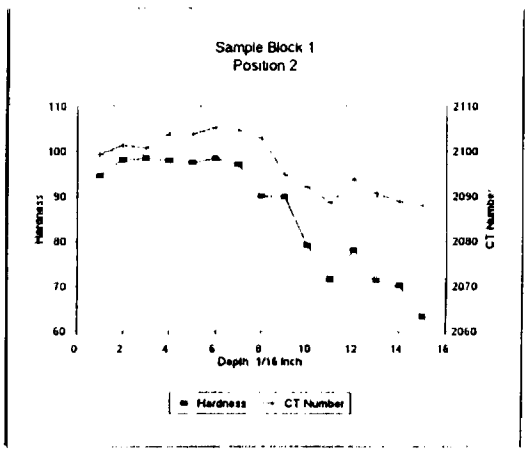

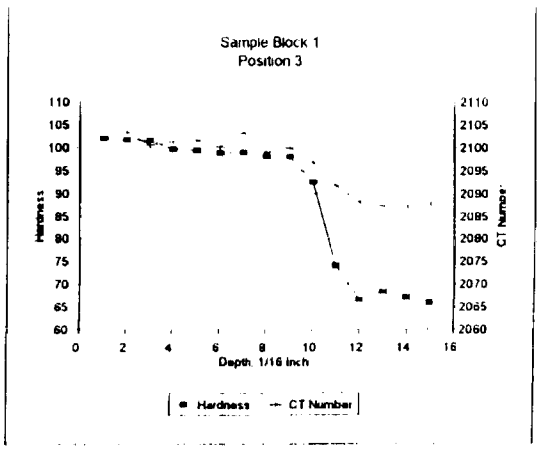

Sample	2
Position	1

Depth	Hard	CT
1	99.5	2102.33
2	99.3	2102.88
3	99.9	2104.00
4	100.8	2104.55
5	100.9	2103.55
6	100.3	2104.22
7	99.9	2101.66
8	98.7	2101.11
9	98.4	2100.33
10	92.1	2095.55
11	82.7	2090.22
12	77.9	2087.66
13	88.5	2085.44
14	89.1	2085.55
15	89.1	2082.22

Sample	2
Position	2

Depth	Hard	CT
1	96.3	2106.77
2	98.0	2107.00
3	98.2	2108.77
4	96.9	2108.66
5	97.9	2108.77
6	97.4	2106.33
7	97.5	2103.11
8	97.4	2104.55
9	94.1	2101.22
10	83.8	2095.33
11	81.3	2094.00
12	87.0	2090.00
13	89.2	2091.22
14	89.4	2088.33
15	87.2	2087.22

Sample	2
Position	3

Depth	Hard	CT
1	96.3	2105.22
2	98.6	2104.11
3	97.6	2106.44
4	97.3	2104.44
5	96.5	2104.66
6	98.0	2103.55
7	96.0	2101.88
8	95.1	2100.00
9	95.6	2099.11
10	94.1	2097.11
11	82.0	2091.33
12	75.3	2086.77
13	81.6	2086.88
14	84.2	2086.44
15	91.3	2086.77

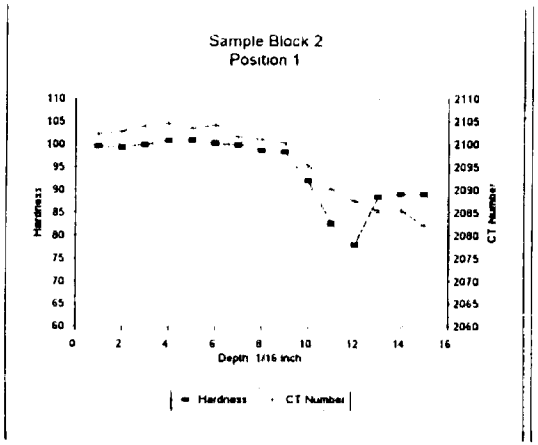

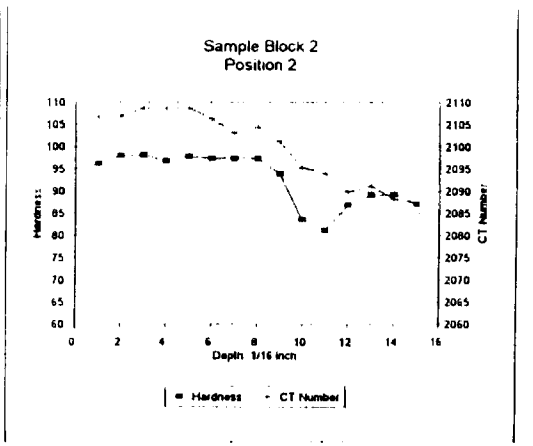

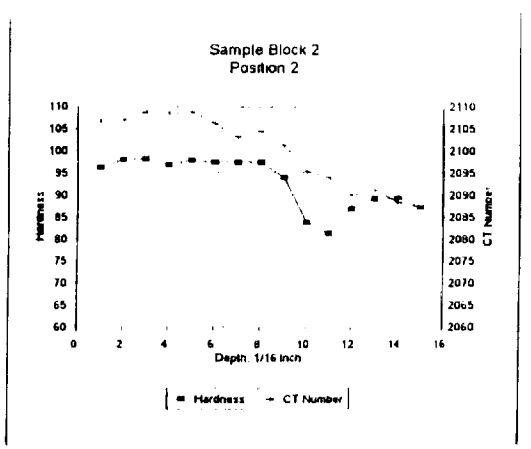

APPENDIX C

Surface 2
Map 1

Depth	Hard	CT
1	91.4	2060.22
2	91.3	2059.56
3	91.4	2060.00
4	87.4	2061.00
5	87.9	2060.78
6	87.9	2060.00
7	86.2	2060.67
8	82.6	2061.11
9	81.7	2061.11
10	77.8	2060.00
11	80.5	2059.11
12	79.0	2058.78
13	74.3	2058.22
14	69.3	2055.89
15	55.2	2053.22
16	48.0	2049.44
17	53.8	2048.78
18	46.8	2043.67

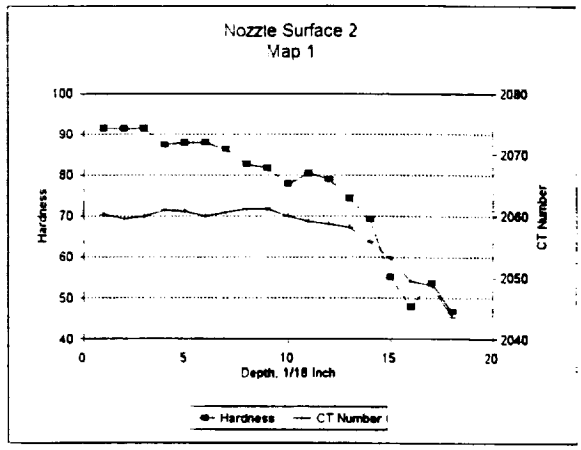

Surface 2
Map 2

Depth	Hard	CT
1	94.6	2069.67
2	94.3	2068.78
3	93.3	2066.44
4	93.5	2068.44
5	92.9	2068.11
6	87.9	2068.11
7	88.7	2066.56
8	87.8	2066.67
9	91.0	2065.33
10	89.6	2066.67
11	86.9	2064.67
12	87.2	2064.67
13	84.3	2064.67
14	82.4	2065.33
15	76.6	2062.00
16	61.3	2059.67
17	59.3	2055.89
18	62.8	2053.78
19	62.5	2052.00

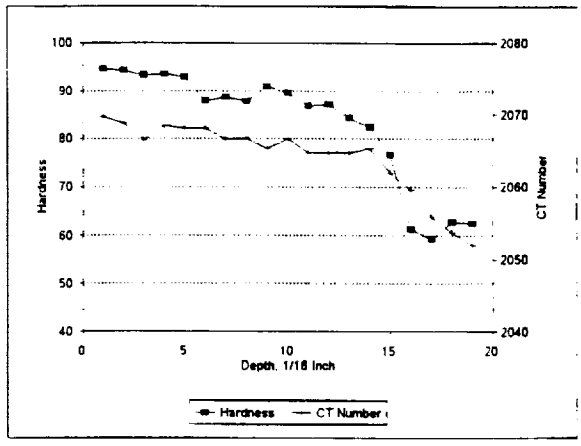

Surface 2
Map 3

Depth	Hard	CT
1	94.1	2070.78
2	93.8	2070.78
3	93.5	2070.44
4	91.1	2069.22
5	92.2	2068.89
6	91.4	2068.00
7	92.2	2067.89
8	91.1	2068.67
9	91.5	2067.44
10	90.5	2066.22
11	88.0	2066.56
12	88.7	2064.78
13	87.0	2065.44
14	86.0	2062.11
15	68.5	2057.56
16	61.4	2057.11
17	67.3	2055.67
18	61.2	2053.56

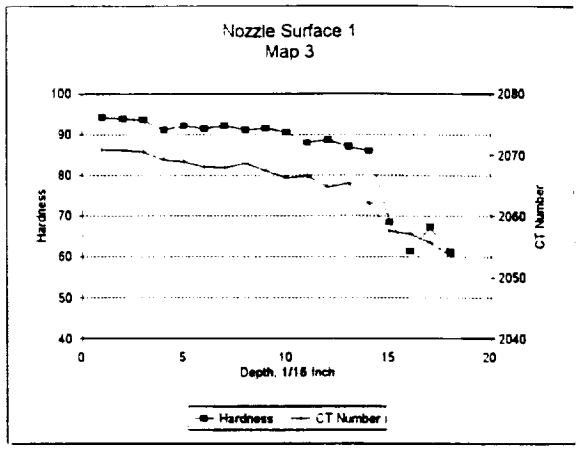

Surface 2
Map 4

Depth	Hard	CT
1	89.6	2071.56
2	94.0	2070.00
3	93.3	2070.11
4	94.6	2070.00
5	94.6	2068.33
6	93.5	2068.89
7	94.8	2067.22
8	94.9	2068.56
9	88.7	2067.78
10	88.8	2065.56
11	88.8	2066.11
12	88.1	2065.22
13	85.0	2064.33
14	76.0	2062.33
15	65.4	2061.11
16	71.2	2058.33
17	74.4	2058.56
18	58.6	2054.00

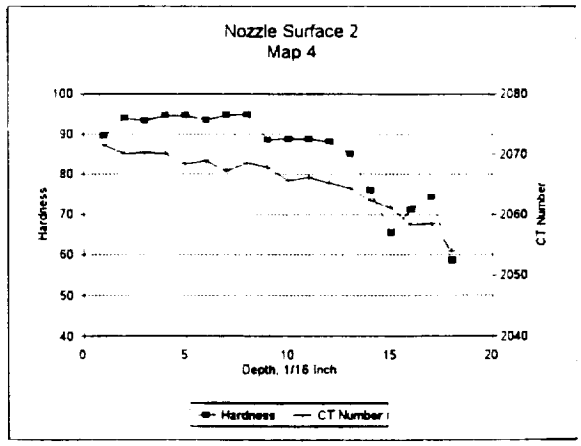

Surface 2
Map 5

Depth	Hard	CT
1	94.2	2067.11
2	92.1	2066.00
3	93.3	2064.67
4	94.1	2065.56
5	94.1	2065.22
6	94.0	2065.89
7	93.4	2064.67
8	92.6	2064.33
9	91.8	2063.78
10	90.8	2063.33
11	86.7	2062.67
12	73.5	2057.11
13	68.4	2056.56
14	71.0	2055.89
15	74.7	2054.44
16	68.4	2053.22

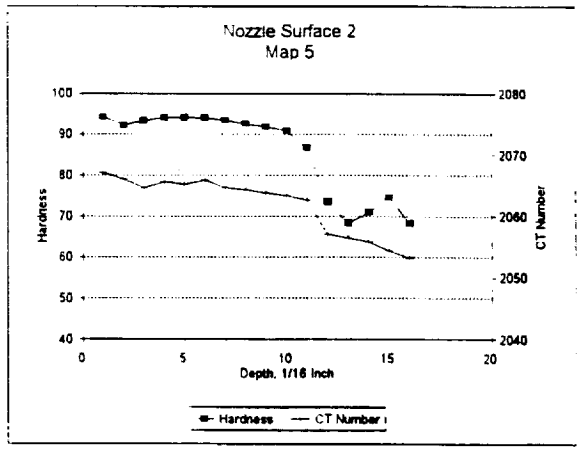

Surface 3
Map 1

Depth	Hard	CT
1	95.1	2060.11
2	94.9	2060.89
3	93.6	2059.67
4	93.9	2059.78
5	93.8	2060.78
6	93.2	2060.67
7	92.8	2060.11
8	92.9	2060.11
9	90.0	2059.78
10	89.1	2059.56
11	86.6	2059.33
12	83.9	2058.33
13	82.6	2058.33
14	76.7	2057.11
15	55.0	2052.33
16	56.0	2047.78
17	60.9	2048.33
18	53.6	2045.00

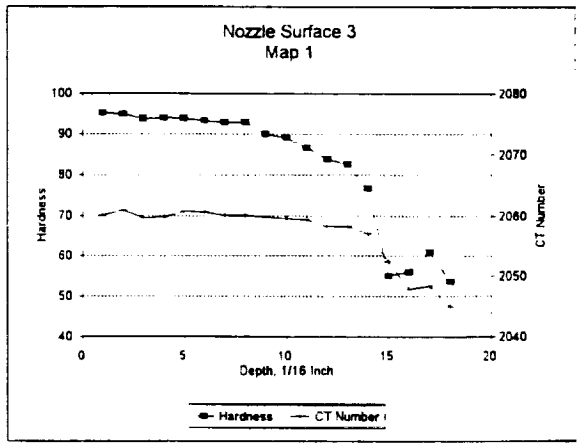

Surface 3
Map 2

Depth	Hard	CT
1	94.8	2070.33
2	94.4	2068.33
3	93.6	2068.44
4	95.2	2067.67
5	93.4	2068.22
6	94.3	2067.78
7	93.9	2066.67
8	93.8	2068.11
9	93.7	2067.44
10	92.4	2067.11
11	91.8	2065.67
12	90.0	2065.00
13	89.5	2066.44
14	87.6	2064.78
15	83.1	2064.56
16	74.6	2061.22
17	67.1	2057.89
18	73.4	2052.89
19	73.9	2052.89

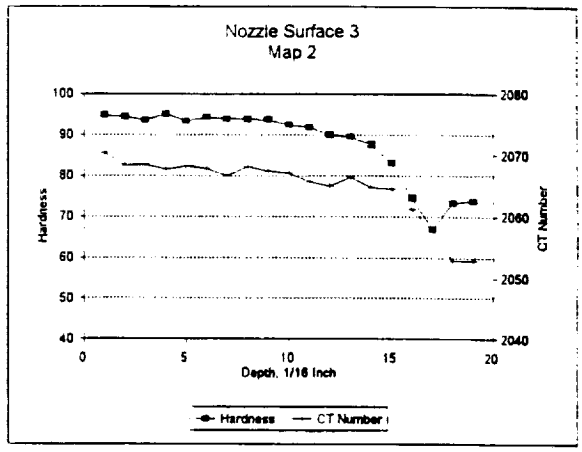

Surface 3
Map 3

Depth	Hard	CT
1	93.1	2072.89
2	93.3	2069.78
3	93.8	2070.22
4	94.8	2071.33
5	94.1	2070.00
6	93.9	2070.00
7	93.8	2068.89
8	92.6	2069.00
9	93.9	2068.44
10	94.6	2067.67
11	90.8	2067.44
12	90.9	2065.44
13	89.5	2065.89
14	86.6	2066.44
15	78.5	2065.00
16	66.7	2061.11
17	68.9	2058.00
18	76.7	2057.33
19	66.8	2053.78

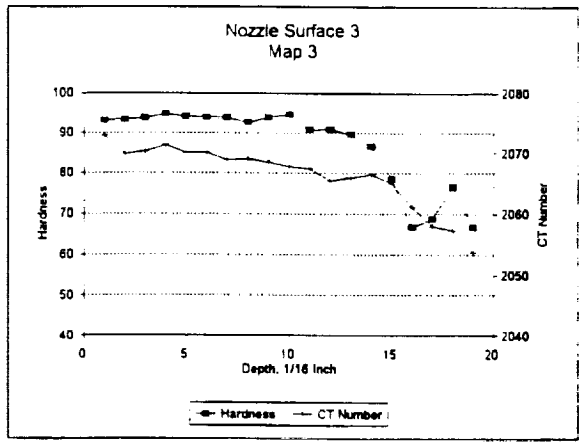

Surface 3
Map 4

Depth	Hard	CT
1	90.7	2071.22
2	91.3	2069.33
3	92.3	2070.67
4	93.2	2069.67
5	93.2	2069.78
6	93.3	2068.44
7	93.1	2068.22
8	92.9	2068.33
9	91.5	2067.89
10	90.4	2068.11
11	91.3	2066.89
12	88.4	2066.44
13	86.5	2066.67
14	77.7	2064.67
15	67.0	2061.00
16	77.0	2059.00
17	74.6	2056.22
18	62.3	2054.00

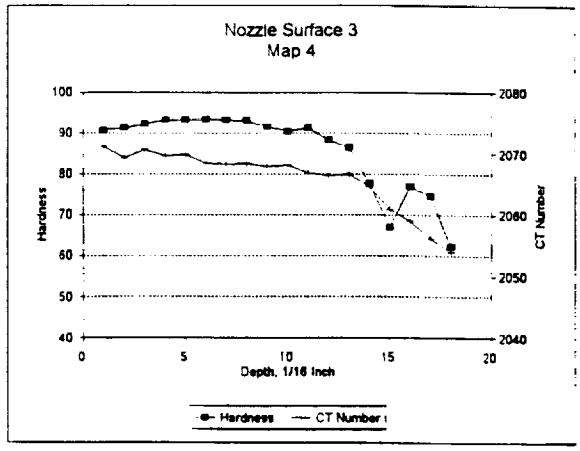

Surface 3
Map 5

Depth	Hard	CT
1	87.3	2066.33
2	89.6	2066.78
3	87.1	2066.33
4	91.3	2065.44
5	91.2	2066.67
6	91.4	2066.67
7	91.9	2066.44
8	89.8	2064.56
9	90.6	2065.33
10	89.5	2065.33
11	87.6	2064.00
12	76.7	2058.78
13	68.0	2057.67
14	71.3	2057.56
15	79.3	2054.22
16	70.0	2049.44

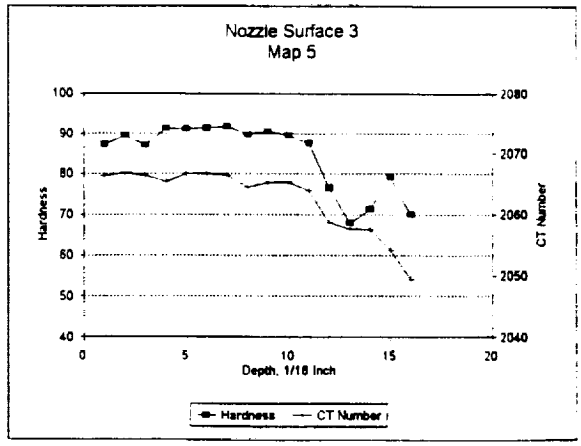

Surface 4
Map 1

Depth	Hard	CT
1	93.8	2066.89
2	94.9	2065.11
3	94.8	2063.89
4	93.0	2063.56
5	94.7	2063.67
6	94.6	2064.44
7	92.5	2063.11
8	94.1	2063.56
9	94.0	2062.11
10	94.6	2062.56
11	89.7	2061.67
12	90.3	2061.78
13	90.6	2061.67
14	90.1	2059.22
15	86.5	2057.00
16	73.8	2052.00
17	59.3	2051.44
18	67.1	2048.00
19	69.6	2045.56

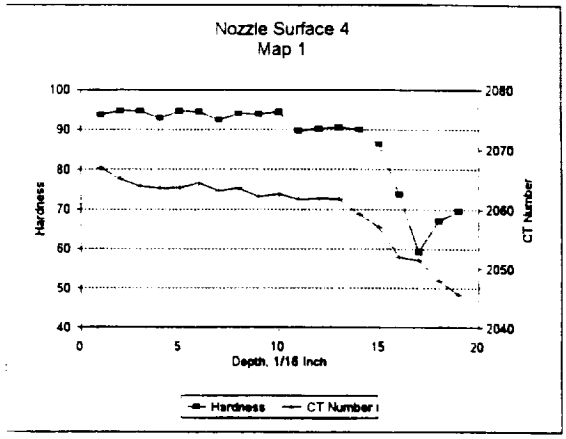

Surface 4
Map 2

Depth	Hard	CT
1	94.9	2069.78
2	94.8	2069.11
3	94.5	2068.44
4	94.6	2068.33
5	95.3	2066.89
6	95.5	2067.89
7	95.0	2067.89
8	94.0	2067.11
9	95.0	2066.22
10	93.9	2066.67
11	93.6	2065.67
12	93.2	2065.44
13	89.2	2065.11
14	90.1	2063.22
15	85.6	2060.78
16	78.2	2058.22
17	67.9	2053.67
18	65.5	2054.00
19	70.4	2051.00

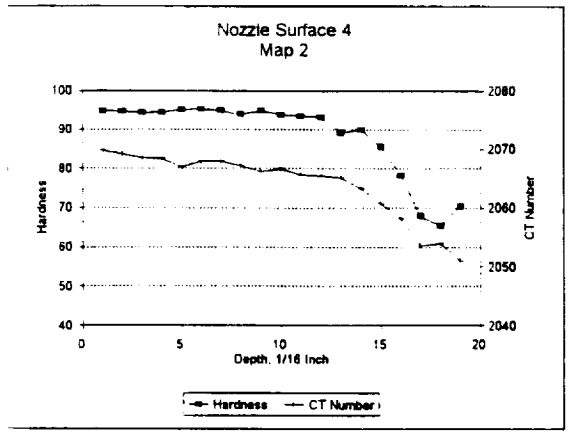

Surface 4
Map 3

Depth	Hard	CT
1	92.8	2073.78
2	94.1	2069.67
3	94.4	2069.22
4	93.1	2069.89
5	94.3	2071.11
6	94.7	2069.56
7	93.4	2068.56
8	91.4	2069.89
9	93.6	2068.00
10	93.0	2068.78
11	91.8	2068.22
12	89.5	2067.00
13	87.6	2066.22
14	85.3	2064.89
15	81.4	2063.44
16	64.0	2057.44
17	59.8	2058.00
18	65.3	2056.00
19	64.2	2053.00

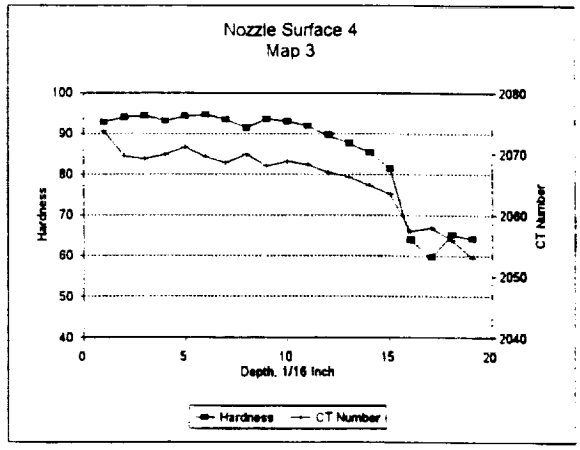

Surface 4
Map 4

Depth	Hard	CT
1	92.8	2070.67
2	92.5	2069.56
3	94.2	2067.67
4	94.4	2069.89
5	94.2	2067.78
6	94.0	2069.44
7	95.3	2067.44
8	93.8	2068.67
9	94.0	2067.78
10	92.6	2068.00
11	90.4	2066.89
12	91.2	2066.00
13	88.5	2064.78
14	82.6	2060.33
15	65.9	2057.22
16	69.3	2056.11
17	73.0	2054.44
18	70.4	2051.56

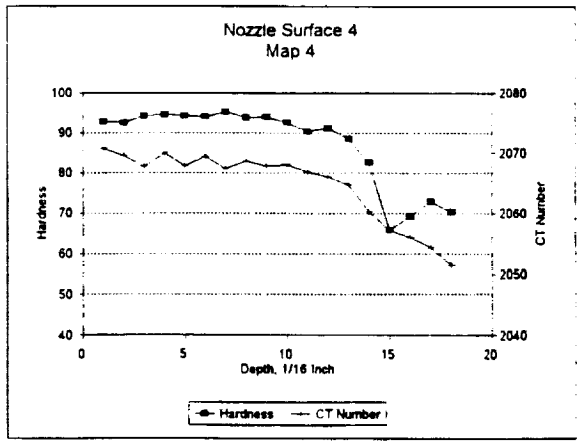

Surface	4
Map	5

Depth	Hard	CT
1	90.6	2069.56
2	90.8	2068.00
3	92.4	2066.22
4	93.5	2066.11
5	94.2	2068.22
6	94.5	2065.00
7	94.4	2065.44
8	94.1	2064.89
9	93.2	2065.56
10	92.3	2064.00
11	91.2	2062.78
12	82.2	2059.33
13	68.5	2058.33
14	69.6	2055.00
15	73.1	2054.44
16	79.7	2051.78
17	71.3	2049.78